AD-A035 377   BOEING AEROSPACE CO SEATTLE WASH RESEARCH AND ENGINE--ETC F/G 9/4
OPTICAL POWER SPECTRUM ANALYSIS OF DISPLAY IMAGERY. PHASE I. CO--ETC(U)
NOV 76   R A SCHINDLER   F33615-76-C-0030

UNCLASSIFIED   AMRL-TR-76-96   NL

1 OF 1
AD-A
035 377

AD-A035 377

OPTICAL POWER SPECTRUM ANALYSIS OF DISPLAY IMAGERY

PHASE I. CONCEPT VALIDITY

BOEING AEROSPACE COMPANY
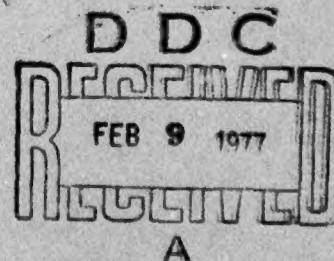
SEATTLE, WASHINGTON

NOVEMBER 1976

AMRL-TR-76-96

OPTICAL POWER SPECTRUM ANALYSIS OF DISPLAY IMAGERY Phase I: Concept Validity

RESEARCH AND ENGINEERING DIVISION
THE BOEING AEROSPACE COMPANY
SEATTLE, WASHINGTON 98124

NOVEMBER 1976

DDC

RECEIVED

FEB 9 1977

A

NOTICES

Please do not request copies of this report from Aerospace Medical Research Laboratory. Additional copies may be purchased from:

> National Technical Information Service
> 5285 Port Royal Road
> Springfield, Virginia 22161

Federal Government agencies and their contractors registered with Defense Documentation Center should direct requests for copies of this report to:

> Defense Documentation Center
> Cameron Station
> Alexandria, Virginia 22314
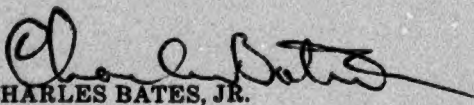
TECHNICAL REVIEW AND APPROVAL

AMRL-TR-76-96

This report has been reviewed by the Information Office (OI) and is releasable to the National Technical Information Service (NTIS). At NTIS, it will be available to the general public, including foreign nations.

This technical report has been reviewed and is approved for publication.

FOR THE COMMANDER

CHARLES BATES, JR.
Chief
Human Engineering Division
Aerospace Medical Research Laboratory

REPORT DOCUMENTATION PAGE		READ INSTRUCTIONS BEFORE COMPLETING FORM
1. REPORT NUMBER AMRL-TR-76-96	2. GOVT ACCESSION NO.	3. RECIPIENT'S CATALOG NUMBER
4. TITLE *(and Subtitle)* OPTICAL POWER SPECTRUM ANALYSIS OF DISPLAY IMAGERY Phase I: Concept Validity		5. TYPE OF REPORT & PERIOD COVERED Interim Report* 3 MAY 1976 - 31 JULY 1976
		6. PERFORMING ORG. REPORT NUMBER
7. AUTHOR(s) Richard A. Schindler		8. CONTRACT OR GRANT NUMBER(s) F33615-76-C-0030
9. PERFORMING ORGANIZATION NAME AND ADDRESS Research and Engineering Division The Boeing Aerospace Company Seattle, Washington 98124		10. PROGRAM ELEMENT, PROJECT, TASK AREA & WORK UNIT NUMBERS 61102F; 2313-VI-15
11. CONTROLLING OFFICE NAME AND ADDRESS Aerospace Medical Research Laboratory, Aerospace Medical Division, Air Force Systems Command, Wright-Patterson Air Force Base, Ohio 45433		12. REPORT DATE November 1976
		13. NUMBER OF PAGES 88
14. MONITORING AGENCY NAME & ADDRESS *(if different from Controlling Office)*		15. SECURITY CLASS. *(of this report)* Unclassified
		15a. DECLASSIFICATION/DOWNGRADING SCHEDULE N/A
16. DISTRIBUTION STATEMENT *(of this Report)* Approved for public release; distribution unlimited		
17. DISTRIBUTION STATEMENT *(of the abstract entered in Block 20, if different from Report)*		
18. SUPPLEMENTARY NOTES * Final report for Phase I.		
19. KEY WORDS *(Continue on reverse side if necessary and identify by block number)* Diffraction Pattern Sampling Display Evaluation Information Theory Optical Power Spectrum		
20. ABSTRACT *(Continue on reverse side if necessary and identify by block number)* A basic approach to the determination of display information capacity using optical power spectrum measurements is examined mathematically and experimentally. While the basic concept is found to be valid, potential problems for practical application are identified. Possible solutions to these problems are considered and promising techniques noted for future study. The potential applicability of the basic approach for display systems evaluation is discussed.		

DD ₁ FORM JAN 73 **1473**   EDITION OF 1 NOV 65 IS OBSOLETE

SUMMARY

PURPOSE

The basic goal of the total study program is to establish the validity,
capabilities and limitations of optical power spectrum measurement for the
determination of visual display information capacity. The purpose of this
initial phase is to establish the validity of the basic concept and ap-
proaches to be used.

APPROACH

The basic measures, transformations and analyses were examined both mathe-
matically and experimentally with respect to the conditions and assumptions
of information theoretic measures of capacity. The basic measurement capa-
bilities of existing equipment were assessed in terms of accuracy and repeat-
ability. Potential problems in practical application were identified and
evaluated. Possible solutions were identified and evaluated as candidates
for further development.

Display performance parameters were reviewed with respect to effects on the
information capacity measure in order to identify measurement requirements
and potential areas of application for display evaluation.

RESULTS AND CONCLUSIONS

The general approach of optical power spectrum measurement for the deter-
mination of display information capacity is valid at the basic level.

The basic measurement capabilities of the existing optical power spectrum
measurement equipment and calibration procedures are adequate. Root-mean-
square (RMS) deviations from theoretical values are about 10%. RMS measures
of repeatability are about 2% of the mean. These values apply over a useful
dynamic range of 6 orders of magnitude.

There are a number of potential problems in the practical application of
the general approach:

> o Nonlinearity of amplitude units
> o Measuring aperture effects

1

o   Phase effects

o   CRT film recording

o   Noise measurement

Promising solutions for these problems exist, but most need further develop-
ment and testing.

The development of the display relationships include both display and viewer
parameters.

o   Spatial frequency response

o   Dynamic range

o   Luminance

o   Visual integration time

o   Input image characteristics

o   Noise

o   Viewing distance

PREFACE

This report was prepared by the Crew Systems organization of the Guidance and Control Engineering portion of the Research and Engineering Division of The Boeing Aerospace Company, Seattle, Washington. The work was done under USAF Contract F33615-76-C-0030, for the Visual Display Systems Branch, Human Engineering Division, of the Aerospace Medical Research Laboratory. Mr. Wayne Martin was the contract monitor for AMRL.

This phase of the study was started in May 1976 and completed in July 1976.

TABLE OF CONTENTS

SECTION I
INTRODUCTION

The Optical Power Spectrum (OPS) is a physical measure that can be used to quantify certain characteristics of display imagery. It is an attractive approach because of its speed and simplicity and because it operates in the frequency domain like its cousin, the modulation transfer function. The latter advantage is especially important when working with displays whose performance is frequency dependent. This is the same for nearly all pictorial displays such as photographs or television receivers.

The OPS measure can be related to such concepts as display information content and capacity as developed by information theorists. Information theory has, for many years, proved to be a valuable tool for the analysis and evaluation of communications systems. Application to pictorial displays has been developing in recent years and promises to be equally useful in this area. The purpose of most displays is to provide information to the viewer. Any display is limited, spatially and temporally, in the amount of information that it can provide. This limit, information capacity, is an important parameter in the evaluation of display quality. Knowledge of the impact of display design parameters on information capacity and of the impact of information capacity on viewer performance is important for effective development and/or selection of displays. The measurement of information capacity is a useful tool for the development of this knowledge.

The objective of the total study effort is to define and validate OPS measurement techniques to determine display information capacity and to apply these techniques to the evaluation of selected display parameter effects on viewer performance. This report covers the initial phase of the study and is concerned with the validity of the basic OPS approach to information capacity measurement. The basic approach is examined both theoretically and experimentally to determine the capabilities and limitations for capacity measurement and to outline potential areas of application. Phase II will develop the specific measurement procedures and apply these to the preliminary

testing of the relationship between the capacity measures and viewer per-
formance. Emphasis will be on CRT displays. Phase III will apply the
resulting procedures for the evaluation of specific display parameter
effects.

SECTION II
DISPLAY INFORMATION CAPACITY

DEFINITION

The information theory approach has provided a useful tool for evaluating
the effectiveness and efficiency of information transmission systems.
Application of the theory to visual displays has received considerable
attention in recent years. Reference 1 provides a good review of this
work. Appendix A of this report provides a brief background of informa-
tion theory and the development of the basic equation for display informa-
tion capacity.

$$C = \frac{N \log_2 L}{D} \qquad (1)$$

where C = capacity (bits per unit display area)
             N = number of independent display elements
             L = number of element response levels
             D = display area.

Equation (1), however, is limited in its application. Few displays of in-
terest have independent display elements (e.g., LED and liquid crystal dis-
plays). The response of a given element on a CRT or photograph, for example,
is influenced by the response levels of neighboring elements. The number of
element response levels is usually not a fixed value but often varies in com-
plicated ways. A matrix of individually illuminated elements can meet the
assumptions of equation (1), i.e., independent elements and fixed number of
response levels. Even here, however, the assumptions may be violated with
respect to the viewer if the viewing distance is great enough or if the illu-
mination levels are at viewing threshold.

A more appropriate definition of "N" results if every display of interest is
defined as "band-limited." That is, there exists a spatial frequency, K, be-
yond which no information is transmitted to the viewer. This limit may be im-
posed by the display (e.g., element spacing) or by the capabilities of the
observer's visual system (i.e., visual acuity). Then, the minimum number
of samples needed to unambiguously specify any given display response is,

$$N = 4K^2D.$$

The factor of 4 is necessary because of the requirement for 2 samples per cycle in each direction. Equation (2) applies to continuous displays such as photographs or along scan lines in CRT displays. Equation (2) also applies to the discrete element case, where, if

$$d = \text{spacing between elements}$$

then $$K = \frac{1}{2d}$$

The factor of 2 in the denominator is necessary because of the requirement for 2 samples per cycle. Determination of the number of response levels, L, is the most difficult and controversial aspect of information capacity measurement. In the simplest cases, L is determined by the characteristics of the display. This is true for an LED matrix display where the elements are either on or off and the illuminated elements are easily perceived by the viewer. Then $L = 2$. In more complex situations, factors such as noise and system frequency response characteristics become important. If the display can provide any output level over a range R_{min} to R_{max} then L can be defined as

$$L = \left[(R_{max} - R_{min}) / \Delta R \right] + 1 \qquad (3)$$

where $\Delta R =$ just discriminable difference in signal response level R.

Equation (3) is in the form of the familiar signal-to-noise ratio. It is strictly valid, however, only if the system is linear, if ΔR is independent of the value of R and if R_{max}, R_{min} and ΔR are constant for all possible display responses. The latter requirement is generally not met by most optical or electronic displays. These displays are usually frequency dependent in their response levels. Highly detailed (high frequency) patterns have a restricted range of allowable response levels compared to gross (low frequency) patterns. This situation requires that capacity be expressed as the integral

8

~f the frequency related L values, so

$$C = 4 \int\int^{K_x \ K_y} \log_2 \left[L(k_x, \ k_y) \right] dk_x \ dk_y. \qquad (4)$$

where k_x and k_y are spatial frequencies in the x and y directions respectively, and K_x and K_y, (the upper limits of integration) are the band-limited cutoff frequencies in the x and y directions.

Determination of the values L $(k_x, \ k_y)$ is simplified if the display response function, R (x, y) is transformed to the frequency domain by using the Fourier transform,

$$F(k_x, \ k_y) = \int\int R(x, y) \ \exp \left[- 2 \ \pi \ i \ (k_x x + k_y y) \right] dx \ dy. \qquad (5)$$

Using the general form of equation (3) we can define

$$L(k_x, \ k_y) = \frac{F_{MAX}(k_x, \ k_y)}{F_{\Delta R}(k_x, \ k_y)} + 1 \qquad (6)$$

where $F_{MAX}(k_x, \ k_y)$ is the Fourier transform of the maximum display response. $F_{\Delta R}(k_x, \ k_y)$ is the Fourier transform of the just discriminable display signal response.

Thus, we can rewrite equation (4),

$$C = 4 \int\int^{K_x \ K_y} \log_2 \left[\frac{F_{MAX}(k_x, \ k_y)}{F_{\Delta R}(k_x, \ k_y)} + 1 \right] dk_x \ dk_y \qquad (7)$$

9

DETERMINATION OF $F_{MAX}(k_x, k_y)$

Information theory demonstrates that $F(k_x, k_y)$ is maximized when the input signal for the display has equi-probable element response levels with zero memory (see Appendix A). This will occur when the input signal is random over a response range that is at least as great as the dynamic range capabilities of the display. $F_{MAX}(k_x, k_y)$, then, can be obtained by providing the appropriate random input to the display and determining the Fourier transform of the resulting display response.

It may also be meaningful to determine capacity for selected classes of input signals such as alphanumeric symbols or aerial photography. It is generally better in such instances to use a measure defined by information theory as "information content."

$$H = CD$$

where

H = information content (bits)
C = capacity (bits/unit area)
D = display area

Then,

$$H = 4D \iint \log_2\left[\frac{F_s(k_x, k_y)}{F_{\Delta R}(k_x, k_y)} + 1\right]dk_x\,dk_y \qquad (8)$$

where

$F_s(k_x, k_y)$ is the Fourier transform of the displayed signal of interest.

DETERMINATION OF $F_{\Delta R}(k_x, k_y)$

The most common approach here is to use the display noise level as the basis for measurement (References 1, 2, 3, 4). The response distribution for a constant level input, $R_N(x, y)$ is Fourier transformed to produce $F_N(k_x, k_y)$ and the assumption made that

$$F_{\Delta R}(k_x, k_y) = F_N(k_x, k_y)$$

10

and, so

$$L(k_x, k_y) = \frac{F_{MAX}(k_x, k_y)}{F_N(k_x, k_y)} + 1$$

This approach assumes that performance is display noise limited. It is strictly valid only for systems that are linear in amplitude and for noise distributions that are signal independent and additive. The effects of deviations from these conditions are not well known.

There are other approaches available. $F_{\Delta R}(k_x, k_y)$ could be determined experimentally for a given display. A psychometric evaluation or, perhaps, existing visual performance data could be used to establish just detectable display response levels $R_{\Delta R}(x, y)$ as a basis for the desired values. This psychometric approach, however, is time-consuming and expensive and the results limited to the specific displays tested. The use of existing data is questionable if significant display noise levels are involved.

A compromise approach is to examine $F_N(k_x, k_y)$ and its effect on viewer performance for display conditions of interest. The objective of such an approach would be to determine if some functional form of the transforms would be a more effective descriptor of display performance, i.e.,

$$L(k_x, k_y) = \left\{ \frac{f\left[F_{MAX}(k_x, k_y)\right]}{g\left[F_N(k_x, k_y)\right]} + 1 \right\}$$

An important tool for this approach will be based on the following multiple regression model,

$$F_{INPUT}(k_x, k_y) = A + B\left[F_S(k_x, k_y)\right] + C\left[F_N(k_x, k_y)\right].$$

Cross spectral correlation will be used to evaluate the functional form and appropriate constants for this model. (See Reference 5 for a similar approach.

The resulting correlational statistics, coefficient of determination and standard error of estimate show promise as indices of display information loss and hence as indirect measures of display information capacity. This approach will be treated in greater detail in Section V.

DYNAMIC DISPLAYS

The determination of $F_S(k_x, k_y)$ and $F_N(k_x, k_y)$ for dynamic displays such as a CRT presents a special problem. The noise response in such instances is properly described as $R_N(x, y, t)$ where t is a time dimension. Furthermore, although we are concerned here only with fixed input signals, the display response includes the effect of noise and will vary with time. Therefore, we must consider $R_S(x, y, t)$ as well. The effect of the dynamic noise component will be modified by the visual integration of the viewer. If T is the visual integration time, then

$$F(k_x, k_y, T) = \iint_{X\,Y} R(x, y, T) \, \exp \left[-2\pi i(k_x x + k_y y) \right] \, d_x d_y \qquad (9)$$

where

$$R(x, y, T) = \int_{t=0}^{T} R(x, y, t) \, dt$$

and

$$C = 4 \iint \log_2 \left[\frac{F_{S,\,N}(k_x, k_y, T)}{F_{\Delta R}(k_x, k_y, T)} \right] \, dk_x \, dk_y. \qquad (10)$$

Note that in the above expression, the numerator $F_{S,N}(k_x, k_y, T)$ includes the effects of noise and the additive factor of 1 is eliminated. Thus,

$$\frac{F_{S,N}(k_x, k_y, T)}{F_{\Delta R}(k_x, k_y, T)} = \frac{F_S(k_x, k_y, T)}{F_{\Delta R}(k_x, k_y, T)} + 1$$

12

SECTION III
OPTICAL POWER SPECTRUM

DEFINITION

The approaches for display information capacity outlined in the previous section all require the determination of the Fourier transform of a display response pattern. This study effort is concerned with the application of a specific technique for such a determination. The optical power spectrum is a physical measurement based on the principles of coherent optical processing. Under proper conditions, an image illuminated with coherent light produces a diffraction pattern having an intensity distribution directly related to the Fourier transform of the input image amplitude transmittance distribution. Specifically under the conditions shown in Figure 1,

$$I(r_x, r_y) = \frac{L^2}{\lambda^2 F^2} \left| F_T(k_x, k_y, T) \right|^2 , \qquad (11)$$

where, $I(r_x, r_y)$ is the diffraction pattern intensity distribution,

r_x, r_y are linear dimensions in the transform plane,

L is the amplitude of the coherent illumination,

λ is the wavelength of the coherent illumination,

F is the focal length of the transform lens,

$\left| F_T(k_x, k_y, T) \right|^2$ is the modulus squared of the Fourier transform of the input amplitude transmittance distribution (after integration over time T).

A description of the physical process and the development of equation (11) is presented in Appendix B.

The optical power spectrum $P(k_x, k_y, T)$ is defined as,

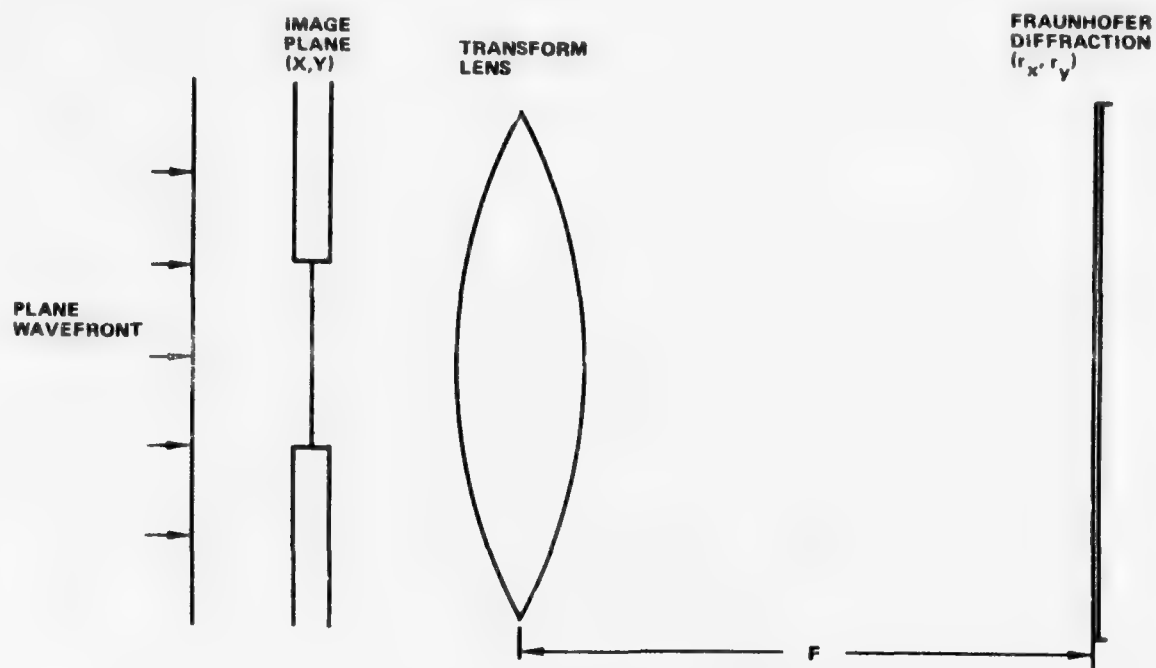$$P(k_x, k_y, T) = \frac{\left| F(k_x, k_y, T) \right|^2}{D} \qquad (12)$$
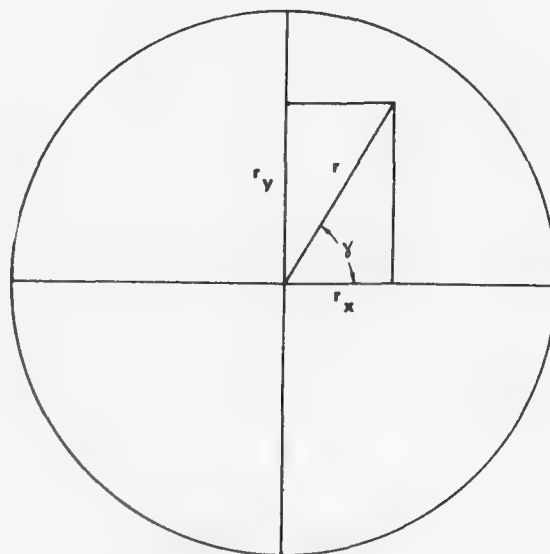
Figure 1: Fraunhofer Diffraction

Figure 2: Polar Units

where, $P(k_x, k_y, T)$ is in units of power per unit frequency squared
　　　D is the area of the input.

Combining equations (11) and (12)

$$P(k_x, k_y, T) = \frac{\lambda^2 F^2}{L^2 D} \ I \ (r_x, r_y, T) \tag{13}$$

It is important to note that the optical power spectrum (and the resulting
capacity measure) is based on the amplitude distribution in the input plane.
This fact has several significant consequences. First, the amplitude
distribution of the display image is probably not the best description of the
display response, R (x, y, T). The visual system responds to intensity (the
square of amplitude) not amplitude. Most visual performance data are based
on intensity, not amplitude units. Furthermore, we can expect linearity prob-
lems, although the same difficulties will exist with intensity since the visual
response is not linear with intensity. The effects of this problem (amplitude
vs. intensity) will be a major concern throughout this study effort.

A second consequence of amplitude dependence is that amplitude is sensitive to
phase effects.   Intensity and the human visual system are not. When film is
used as the input medium, phase shifts may occur because of variation in the
film thickness. (References 6, 7, 8, 9, 10). These effects, if significant,
must be eliminated or minimized.

The third problem is that the power spectrum reflects the distribution of
the total input plane. This includes the effect of any aperture used to
limit the image area being measured. The Fourier transform of the limit-
ing aperture is convolved with the transform of the input image and a simple
correction is not feasible (Reference 9).

It is often convenient to work with polar, rather than linear coordinates,
in the diffraction plane. With the optical axis as the origin, we define
the angle γ and the distance r as shown in Figure 2.   Then

15

$$r_x = r \cos \gamma$$
$$r_y = r \sin \gamma$$

and (11) becomes,

$$I(r, \gamma, T) = \frac{L^2}{\lambda^2 F^2} \left| F(k_r, \gamma, T) \right|^2 . \tag{14}$$

Equation (12) becomes,

$$P(k_r, \gamma, T) = \frac{\left| F(k_r, \gamma, T) \right|^2}{D} . \tag{15}$$

So
$$P(k_r, \gamma, T) = \frac{\lambda^2 F^2}{L^2 D} I(r, \gamma, T). \tag{16}$$

The value of $I(0, 0)$ is of special concern. This value is related to the "DC" or average illuminance value taken over the input plane. From (11)

$$I(0, 0) = \frac{L^2}{\lambda^2 F^2} \left| F(0, 0) \, T \right|^2 .$$

$$F(0, 0, T) = \iint A_T(x, y, T) \exp \left[-2 \pi i (0 + 0) \right] d_x d_y$$

$$= \iint A_T(x, y, T) \, d_x d_y$$

$$= \overline{A}_T \, D$$

where
$\overline{A}_T$ = the average amplitude transmission
D = input image area

and
$$I(0, 0) = \frac{L^2 \overline{A}_T D^2}{\lambda^2 F^2} . \tag{17}$$

From (13)
$$P(0, 0, T) = \frac{\lambda^2 F^2}{L^2 D} I(0, 0)$$

$$= \overline{A}_T^2 \, D \tag{18}$$

16

MEASUREMENT REQUIREMENTS

Equation (16) defines the basic OPS measurement process. The intensity of the diffraction pattern as a function of position must be measured and then multiplied by a constant based on the measurement conditions.

We can separate the required measurement system into several functional areas:

- o Illumination
- o Image control
- o Optical transformation
- o Diffraction Pattern Measurement

Optical considerations and the analytical conclusions derived above define a number of requirements for each of the functional areas.

Illumination

1. The input image must be illuminated with a coherent, collimated source.
2. *The level of illumination must be uniform within the system limiting aperture.*
3. The level of illumination must be consistent with the sensitivity range of input image transmission values.
4. The level of illumination must be stable over reasonable measurement periods.

Image Control

1. The input image must exist in a form capable of varying the illumination amplitude or phase. Only amplitude variation will be used here. Photographic film will be the primary medium. Unwanted phase effects must be controlled.
2. *The image must be positioned so that the system limiting aperture covers the image area of interest.*
3. The image position must be stable throughout the measurement period.
4. The image should be positioned perpendicular to the optical axis of the measurement system. This is not a firm requirement. Deviations will shift the diffraction pattern axes in a predictable manner but optical realignment is required.

Optical Transformation

1. The transform lens should not induce significant aberrations. The lens transfer function should not show a significant drop in response over the spatial frequency range of interest. Transfer effects can be treated analytically; but reduced response levels create signal-to-noise problems in the diffraction pattern measurement.
2. The transform lens focal length should be consistent with the physical size constraints of the system and with the capabilities of the diffraction pattern measurement components. The transform lens focal length determines the "scale" of the diffraction pattern.
3. The transform lens diameter and position must not introduce vignetting over the range of image areas and diffraction angles of interest.

Diffraction Pattern Measurement

1. Diffraction pattern intensity must be measured at the transfer lens focal plane and relatable to position in that plane.
2. The integrating area of the individual sensing elements must be sufficiently large to provide adequate sensitivity and small enough to provide reasonable spatial frequency resolution in the resulting spectra.
3. The dynamic range capabilities of the measurement system must be adequate for the expected intensity variation in the pattern (up to 5 or 6 orders of magnitude).
4. Accuracy and stability of the intensity measurements must be consistent with acceptable error levels for the resulting spectra.

In addition to the specific requirements above, good optical alignment practices must be followed to insure proper geometry and distribution of the diffraction pattern and to minimize the effects of back reflections and stray light.

18

EQUIPMENT

All optical power spectrum measures in this effort will be made with a Record-
ing Optical Spectrum Analyzer (ROSA) manufactured by Recognition Systems, Inc.
This equipment, shown in Figure 3, is a general purpose instrument designed for
ease and flexibility of optical set-up. The optical components, all with mag-
netic mounts, are positioned on a 72 x 44 inch optical table. A fiberglass
shroud covers the table and components to protect against stray light.

For this work, the equipment is configured generally as shown in Figure 4.
The illumination source is a 7 mw He-Ne laser. Illumination is controlled
with a variable attenuator. The attenuator consists of two opposing glass
wedges that are positioned for the desired transmission without imposing a
significant deviation in the laser light path. The laser beam is expanded
with a microscope objective. The magnification of the objective controls
the degree of expansion which, in turn, is determined by the desired area
of illumination at the input plane. A 25 μm pinhole is placed at the focal
point of the microscope objective to "clean up" the laser beam. The laser
and microscope objective can be considered as a crude spectrum analyzer. The
pinhole is placed at the Fraunhofer diffraction plane of the objective and
thus passes only the uniform energy in the laser beam. It acts as a spatial
filter that blocks the high frequency variation in the beam. The expanding
beam is then collimated with a lens placed at a distance from the pinhole
equal to its focal length. A 15-inch focal length telescope objective is gen-
erally used for collimation. During alignment, collimation is assured by
inserting an optical flat in the beam "downstream" from the collimating lens
and adjusting the lens focus until the resulting interference fringes are
minimized.

From the collimating lens, the beam passes through the film holder. This
holder is designed to accept roll film up to 9 inches in width as well as
slides or film "chips." It is equipped with a variable aperture to control
the area illuminated. A series of discrete circular apertures with diameters
from 1/8 inch to 2 and 1/2 inches is available. The holder includes a pro-
jection unit for viewing the illuminated image. This unit is used to aid in
positioning the image in the laser beam.

Figure 3: Recording Optical Spectrum Analyzer

AMPLIFIERS, BCD CONVERTER, POWER SUPPLIES

LASER

VARIABLE ATTENUATOR

SPATIAL FILTER

COLLIMATING LENS
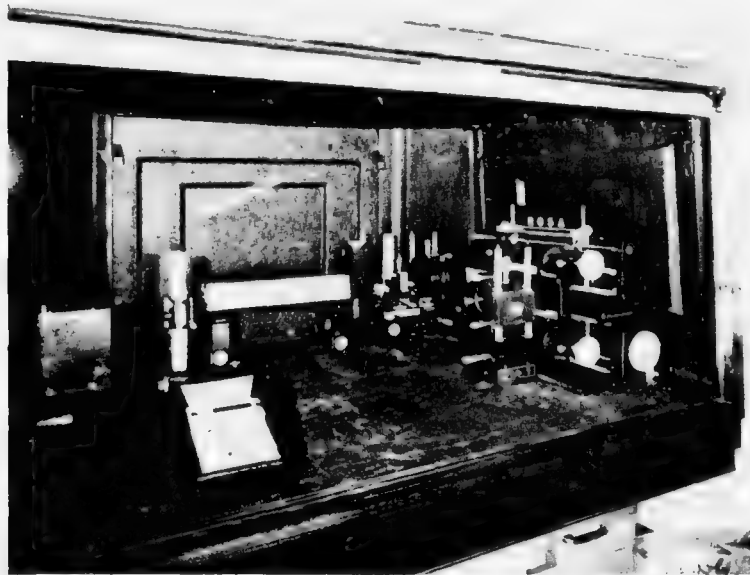
VARIABLE APERTURE

FILM TRANSPORT

CHIP HOLDER

PROJECTION VIEWER
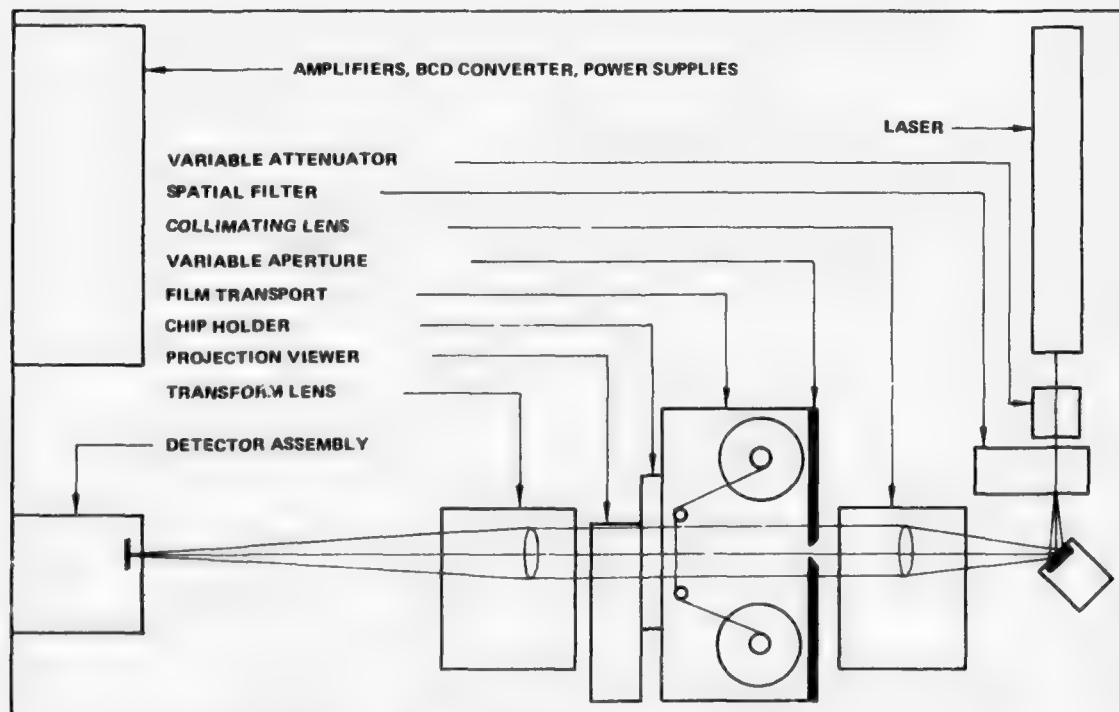
TRANSFORM LENS

DETECTOR ASSEMBLY

Figure 4: Optical Configuration

The light diffracted by the input image is collected by the transform lens and focused on the photodetector. The transform lenses used here are simple spherical telescope objectives. The transform lens focal length determines the distance between the lens and the detector and hence the "scale" of the diffraction pattern.

The ROSA uses a 64 element photodetector array for measurement of the diffraction pattern intensity values. Each element is a diffused silicon photodetector on a common substrate. The array as diagrammed in Figure 5 consists of 32 "rings" and 32 "wedges." The diffraction pattern is symmetric so the array is split essentially in half, each half measuring a different "characteristic" of the pattern. The rings measure intensity as a function of frequency integrated over direction and the wedges measure intensity as a function of direction integrated over frequency. The central ring (Ring 1) is a complete circle and measures the pattern "DC" level. The succeeding rings are nearly half circles and provide measures of intensity integrated over a frequency band. Thus

$$I(\text{Ring } i) = \int_{0}^{\Psi_i} \int_{m_i}^{n_i} I(r, \gamma) \; dr \; d\gamma \tag{19}$$

where m_i, n_i = minimum and maximum radii of ring i respectively

Ψ_i = angle covered by Ring i

r, γ are polar coordinates in the diffraction plane.

The lowest and highest frequencies, a_i and b_i, covered by Ring i are determined from equation

$$a_i = m_i/\lambda F$$
$$b_i = n_i/\lambda F$$

21
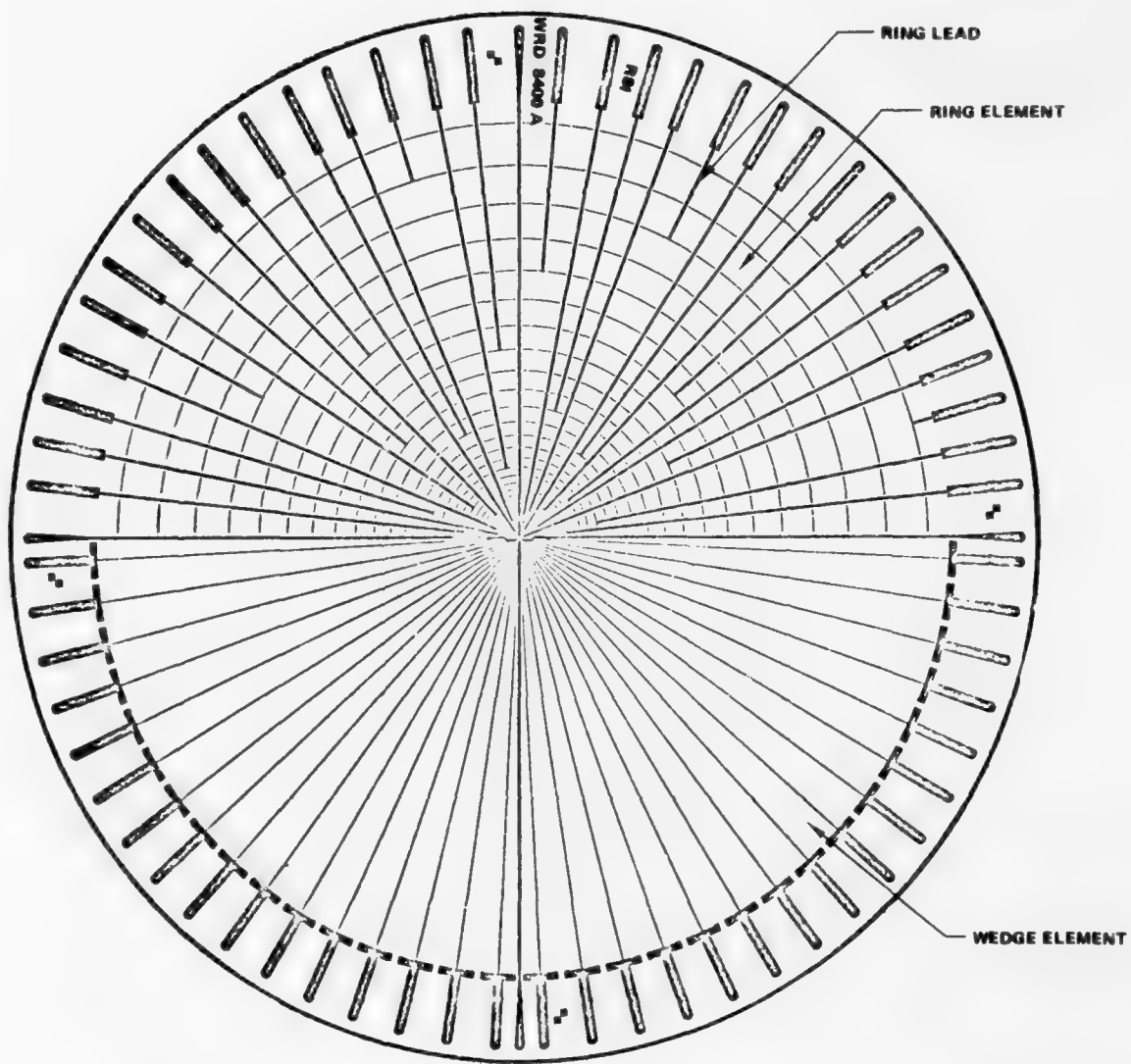
Figure 5: Photodetector Array

where λ = laser wavelength

          F = transform lens focal length

Values for m_i, n_i, Ψ_i and total ring area are listed in Table 1. A 0.8 mil wide conductor strip is incorporated in each ring to improve detector performance. The effect of this strip on total ring effective area is included in the tabled values.

Table 2 shows the corresponding spatial frequency values for the 40 inch transform lens used in this study.

Table 1: Detector Ring Dimensions

Ring No.	Minimum Radius (M_i) (mils)	Maximum Radius (N_i) (mils)	Ring Angle (ψ_i) (degrees)	Total Effective Area (A_i) (sq. mils)
1	0	3.5	360.0	38.5
2	5.8	8.6	180.0	43.5
3	9.6	12.5	180.0	69.1
4	13.5	16.4	180.0	93.5
5	17.4	20.4	180.0	122.7
6	21.4	24.6	166.3	148.6
7	25.6	29.0	168.5	190.0
8	30.0	33.7	170.1	245.0
9	34.7	38.8	171.4	318.7
10	39.8	44.4	172.5	417.4
11	45.4	50.6	173.4	548.7
12	51.6	57.5	174.2	722.0
13	58.5	65.2	174.9	948.7
14	66.2	74.0	175.5	1279.6
15	75.0	83.9	176.0	1688.8
16	84.9	95.1	176.5	2237.0
17	96.1	107.8	176.9	2963.6
18	108.8	122.1	177.3	3884.7
19	123.1	138.3	177.6	5114.3
20	139.3	156.6	177.9	6697.1
21	157.6	177.2	178.1	8715.4
22	178.2	200.2	178.3	11209.0
23	201.2	225.9	178.5	14385.5
24	226.9	254.7	178.7	18473.4
25	255.7	286.7	178.8	23448.5
26	287.7	322.2	179.0	29630.1
27	323.2	361.6	179.1	37361.6
28	362.6	405.0	179.2	46614.1
29	406.0	452.8	179.3	57988.0
30	453.8	505.4	179.3	71889.4
31	506.4	563.0	179.4	88448.7
32	564.0	626.0	179.5	108409.8

Table 2: Detector Spatial Frequency Values

40 inch Focal Length

Ring No.	Minimum Frequency (cy/mm)	Maximum Frequency (cy/mm)	Center Frequency (cy/mm)	Bandwidth (cy/mm)
1	0.00	0.14	0.07	.14
2	0.23	0.34	0.28	.11
3	0.38	0.49	0.43	.11
4	0.53	0.65	0.59	.12
5	0.69	0.80	0.75	.11
6	0.85	0.97	0.91	.12
7	1.01	1.15	1.08	.14
8	1.18	1.33	1.26	.15
9	1.37	1.51	1.44	.14
10	1.57	1.75	1.66	.18
11	1.79	2.00	1.89	.21
12	2.03	2.27	2.15	.24
13	2.31	2.57	2.44	.26
14	2.61	2.92	2.76	.31
15	2.96	3.31	3.13	.35
16	3.35	3.75	3.55	.40
17	3.79	4.25	4.02	.46
18	4.29	4.81	4.55	.52
19	4.85	5.45	5.15	.60
20	5.49	6.17	5.83	.68
21	6.22	6.99	6.60	.77
22	7.03	7.90	7.46	.87
23	7.93	8.91	8.42	.98
24	8.95	10.05	9.49	1.10
25	10.08	11.31	10.69	1.23
26	11.34	12.70	12.02	1.36
27	12.75	14.26	13.50	1.51
28	14.30	15.97	15.13	1.67
29	16.01	17.85	16.93	1.84
30	17.89	19.93	18.91	1.96
31	19.97	22.20	21.08	2.23
32	22.24	24.68	23.46	2.44

The "wedges" are identical except for the two middle ones (Wedges 16 and 17 numbering clockwise). All wedges measure over an included angle of 5.625 degrees. All have an outer radius of 626 mils. Wedges 16 and 17 have an inner radius of 26 mils, the others of 21.4 mils. The total effective area of wedges 16 and 17 is 1748.8 square mils and that of the other wedges it is 1795.9 square mils.

Intensity values for the wedges are given by,

$$I(\text{Wedge } i) = \int_{\alpha_i}^{\beta_i} \int_{m_i}^{n_i} I(r, \gamma) \, dr \, d\gamma, \tag{20}$$

where, α_i, β_i are minimum and maximum angles of wedge i respectively,

m_i, n_i are minimum and maximum radii of ring i respectively.

The outputs from the individual elements are fed into a pre-amp/multiplexer, then each signal is fed into an auto-ranging amplifier where it is converted to the proper range for the binary-coded decimal converter. The signals, converted into 3 digit binary-coded decimals are then recorded on punched cards by a Univac Model 1710 card punch and interpreter. The output values represent microvolts with a maximum value of 1×10^7 μv. Each card contains a 6 digit designator and the output values for 8 elements. Eight cards are produced for each measurement. Time for the measurement sequence, after image positioning, is paced by the key punch and takes about 20 seconds. The data taking procedure is controlled with the entry and control panel. This unit enables the manual entry of the 6 digit designator code for recording on the punched cards.

Data processing for converting the raw voltages to the appropriate power values is accomplished with a Hewlitt Packard Model 9820 calculator. The calculator is equipped with a card reader for data input, an expanded tape memory, and a plotter and typewriter for data output.

DATA PROCESSING

The specific processing techniques to be used depend on the nature of the input image. If the input variation is one-dimensional such as a single slit or a line grid, most of the diffracted energy is confined to a single spike and the power spectrum is properly expressed as one-dimensional (power per cycle/mm). If the image information is truly two-dimensional, then processing must yield the two-dimensional power spectrum (power per $(\text{cycle/mm})^2$.

One-Dimensional Variation

The individual ring voltage values are converted to relative intensity per mil after correction for amplifier bias errors. Bias error values are determined with a dark current (covered detector) reading and subtracted from the element voltages. Relative intensity is determined by dividing by the element width as determined from Table 1. Except for ring 1, the elements must be corrected for the .8 mil conductor strip along each ring. So,

$$I_i(A) = \frac{V_i - B_i}{m_i - n_i - 0.8}, \qquad (21)$$

where

$I_i(A)$ = relative intensity per mil for ring i,

V_i = raw voltage output for ring i

B_i = dark current value (bias correction) for ring i,

n_i, m_i = maximum and minimum radii, respectively, for ring i.

Then, except for ring 1,

$$P(k_r, T) = 2\lambda F I_i(A) = \frac{2\lambda F(V_i - B_i)}{m_i - n_i - 0.8}, \qquad (22)$$

where,

F = the focal length of the transform lens (mils),

λ = the wavelength of the laser

(6.328 x 10^{-4} mm/cycle for the He-Ne laser),

k_r = the center frequency for ring i

(see Table 2).

27

The value 2 is included since the rings 2 through 32 cover only half of the total pattern. Ring 1 is a full circle and does not contain a conductive strip. The center frequency for Ring 1 is considered to be zero. Thus,

$$P(0, T) = \lambda F \ I_i(A) = \frac{\lambda F(V_i - B_i)}{n_i} \ . \tag{23}$$

Equations (21), (22), and (23) provide relative values in that they do not include the effects of laser amplitude or image area as required by equation (16). This is generally solved by normalizing to P(0, T).

$$P'(k_r, T) = \frac{P(k_r, T)}{P(0, T)} = \frac{\dfrac{2(V_i - B_i)}{m_i - n_i - .8}}{\dfrac{(V_1 - B_1)}{n_1}} \ . \tag{24}$$

The prime designation is used, hereafter, to designate the normalized power values. Normalization by the ring 1 value, although a common practice, is not always desirable. First, the normalization eliminates the influence of the average image transmission level. This effect may well be of interest in some applications. Second, the normalization should, theoretically, be made to the true "DC" level or the intensity at zero frequency. Since ring 1 is of finite area, it includes the effects of very low frequencies as well, and thus is only an approximation of the true "DC" level. Selection of the best normalization technique will remain a major concern throughout this study effort.

The wedges are not of direct value in the one-dimensional analysis except to verify the appropriateness of one-dimensional processing. The wedge at the spike orientation should be significantly greater than the general level.

Two-Dimensional Variation

Processing is extended to the two-dimensional input by using the element area and squaring the λF correction factor.

$$P(k_r, T) = \frac{\lambda^2 F^2 (V_i - B_i)}{A_i} \tag{25}$$

where A_i is the element area as listed in Table 1. These values include the compensation for the conductive strip and for the variation in angular coverage of the rings so the factors of 2 and 0.8 used in equation (22) are not required and equation (25) applies to all rings including ring 1.

Normalization to ring 1 provides,

$$P'(k_r, T) = \frac{P(k_r, T)}{P(0, T)} = \frac{\dfrac{(V_i - B_i)}{A_i}}{\dfrac{V_1 - B_1}{A_1}} . \tag{26}$$

Processing for the wedge data is complicated by the reduced areas in wedges 16 and 17. Area correction is not appropriate here since this correction assumes an equal energy distribution across the element. This is usually an acceptable assumption for the rings in the two-dimensional analysis but does not hold for the wedges. Standard processing techniques for the wedge elements have not been established.

Visual Angle Transformations

When the power spectrum is to be related to visual performance, units relating to visual angle are preferred. This is accomplished by the use of the following relationship.

$$k_\theta = \frac{k_r}{\arctan(1/D)} , \tag{27}$$

where, k_θ = spatial frequency in cycles/degree
            D = viewing distance in millimeters
            k_r = spatial frequency in cycles/millimeter

and,

29

$$P^{\prime}(k_{\theta}, T) = \frac{P^{\prime}(k_r, T)}{[\arctan{(1/D)}^2]} \tag{28}$$

where $P^{\prime}(k_{\theta}, T)$ is in units of relative power per $(\text{cycle/degree})^2$.

Intermediate Image Scale

The optical power spectrum measurement requires that the input image exist as a transparency. Measurement of CRT display imagery, for example, will require the use of a photograph of the screen. The scale of this intermediate image must be used to adjust the dimensions of the measured spectrum to refer to the original display dimensions.

SECTION IV
EXPERIMENTAL TESTS

INTRODUCTION

This section describes a series of tests designed to provide experimental
demonstrations of the general validity of the basic approaches described
in the previous sections. The tests are not intended as an evaluation of any
specific technique for the measurement of image information capacity. Results
can, at best, indicate the potential for practical application of the approach
described in this report. Evaluation of specific practical techniques is the
subject of Phase II in this study effort.

BASIC POWER SPECTRUM MEASURES

The validity of the basic diffraction integral (equation 11) can be examined
by considering simple apertures as input images. This is a useful starting
point since a simple clear aperture in opaque material represents the total
input distribution. There are no additional limiting aperture effects and
no phase effects. Transmittance levels are 0 and 1 and so provide the special
situation where amplitude and intensity are equal. Comparison of measured with
theoretical clear aperture values provides an indication of the magnitude of
the errors that may exist in the practical application of the theory. The
principal sources of error here are in

1) The quality and alignment of the optics,

2) The accuracy and sensitivity of the photodetector and electronics,
   and

3) The accuracy and effectiveness of the data processing and calibra-
   tion techniques.

One Dimensional Variation

We can express the definition of the power spectrum from equation (12) in
one dimension as,

31

$$P(k_x, T) = \frac{\left| F(k_x, T) \right|^2}{\omega}$$

where

$$F(k_x, T) = \int R(x, T) \exp \left[-2\pi i k_x x \right] dx$$
$$\omega = \text{size of the image in the direction of interest } (x).$$

The simplest case of a one-dimensional measurement is a single long slit. Consider a clear slit of width, ω, placed symmetrically about the origin and uniformly illuminated so that the response function

$$R(x, T) = \begin{cases} 1 \text{ for } \left| x \right| \leq \omega/2 \\ 0 \text{ elsewhere} \end{cases}$$

Since the aperture is time invariant, the T designation will be dropped. Over the area of integration,

$$R(x) = 1$$

and,

$$F(k_x) = \int_{-\omega/2}^{+\omega/2} \exp (-2\pi i k_x x) kx = -\frac{1}{2\pi i k_x} \left[\exp (-2\pi i k_x x) \right]_{-\omega/2}^{+\omega/2}$$
$$= \frac{\sin (\pi k_x \omega)}{\pi k_x \omega} .$$

Thus

$$P(k_x) = \left(\frac{\sin(\pi k_x \omega)}{\pi k_x \omega} \right)^2$$

and

$$P'(k_x) = \frac{P(k_x)}{P(0)} = \frac{\left(\frac{\sin(\pi k_x \omega)}{\pi k_x \omega} \right)^2}{\left(\frac{\sin 0}{0} \right)^2} , \tag{29}$$

32

where $\dfrac{\sin 0}{0}$ is defined as equal to 1.

Figure 6 is a plot of equation (29) for $\omega = 1.5$ mm. Since the power spectrum is proportional to the diffraction pattern intensity, the plot shows the slit diffraction pattern as a line of closely spaced spots decreasing in intensity from the center. With the exception of the center, the spots are spaced 0.67 cycles/mm apart. Since distance in the diffraction plane, r, is,

$$r = F\lambda k_r,$$

the spots will be about 0.017 inches apart in the pattern produced by a 40 inch transform lens.

The finite width of the detector ring elements will integrate the energy over the corresponding distances. The detector thus performs a "smoothing" function in the measurement process. Since the ring widths increase with distance, the smoothing is greater at higher frequencies. Smoothing has the danger of hiding real variations in the pattern,but is useful in averaging out random discrepancies to produce a more stable and representative spectrum. Equation (29) has been integrated over the appropriate frequency ranges for the individual rings, assuming a 40 inch transform lens focal length, and the results shown in Figure 7. The effects of the smoothing process are clearly evident.

Five repeated optical power spectra measurements were made using a 1.5 mm wide slit. The ROSA was configured with a 40 inch focal length transform lens. Mean values were used with equation (24) to provide the data points shown in Figure 8. The solid curve represents the theoretical values constructed by joining the midpoints of the bars in Figure 7. The root mean square error is about 11% of the mean value over the range of more than 4 orders of magnitude. The theoretical values are strictly correct only for a slit that is infinitely long. The slit used here was slightly over 11 mm in length. The length does contribute to the diffraction pattern. The magnitude of this contribution was calculated and found to be 3% or less and has been neglected here. The repeatability of the readings was assessed by calculating the standard deviation for
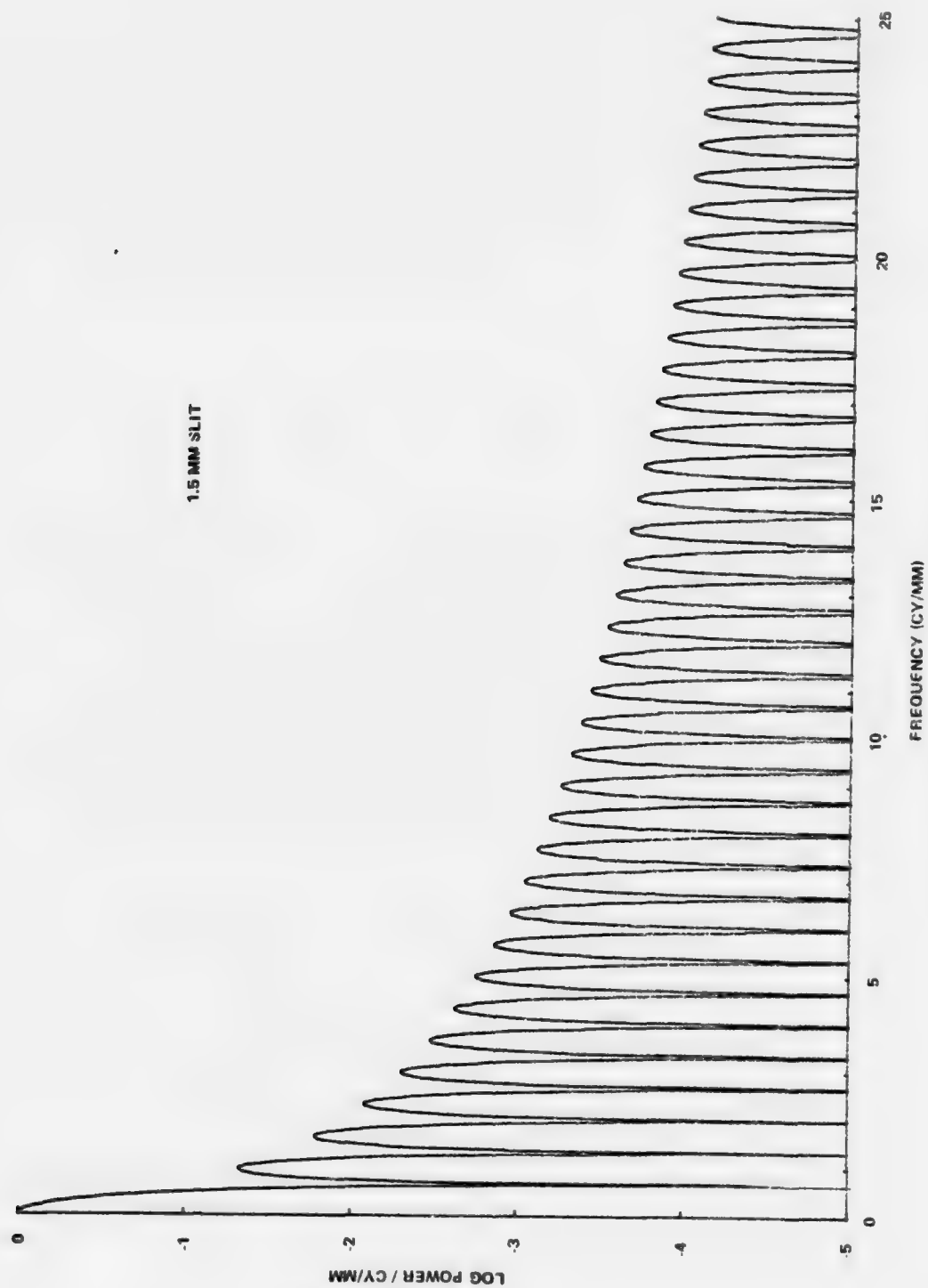
33

1.5 MM SLIT

Figure 6: *Theoretical Spectrum (1.5mm Slit)*

LOG POWER / CY/MM

FREQUENCY (CY/MM)

34

1.5 MM SLIT
40 INCH TRANSFORM LENS

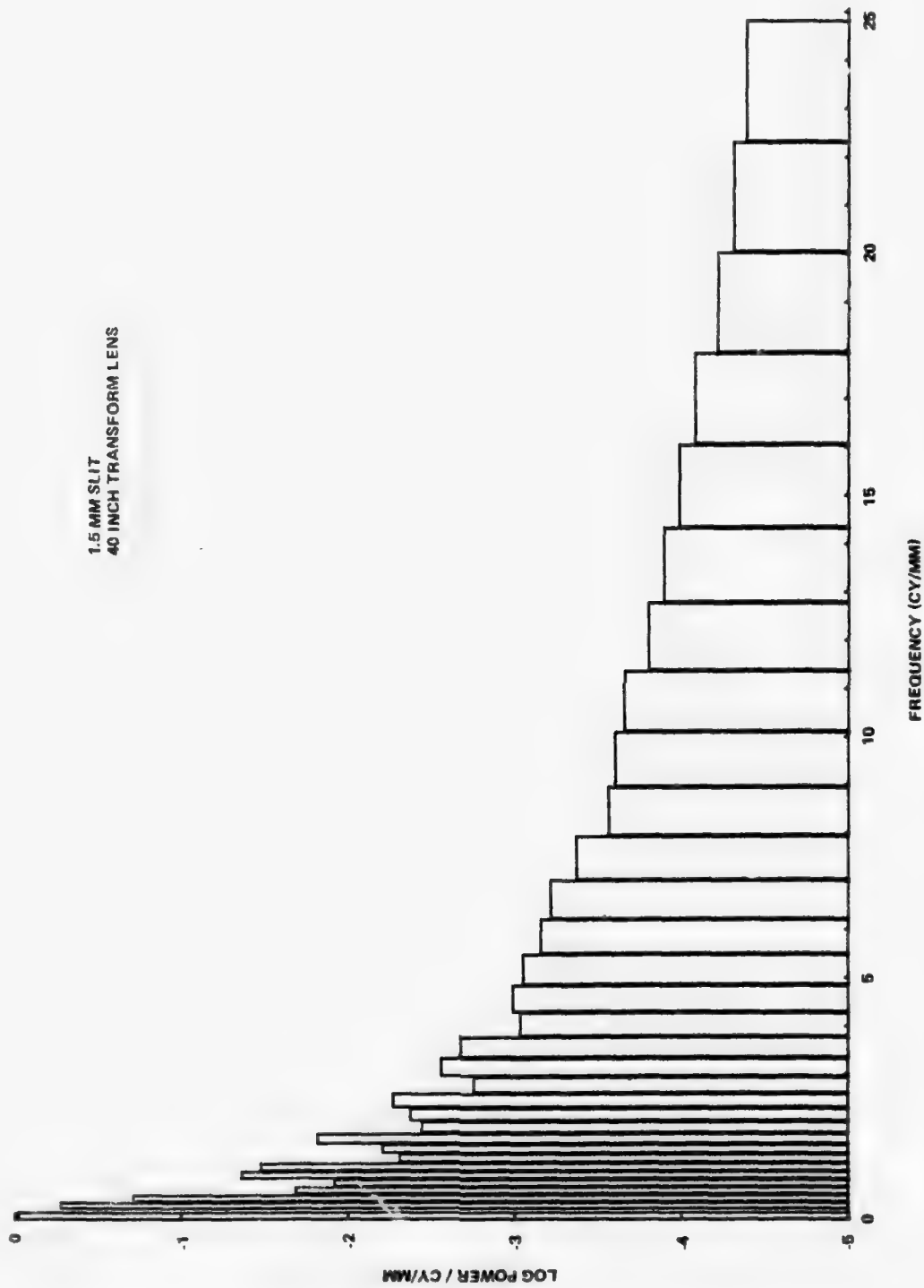LOG POWER / CY/MM

FREQUENCY (CY/MM)

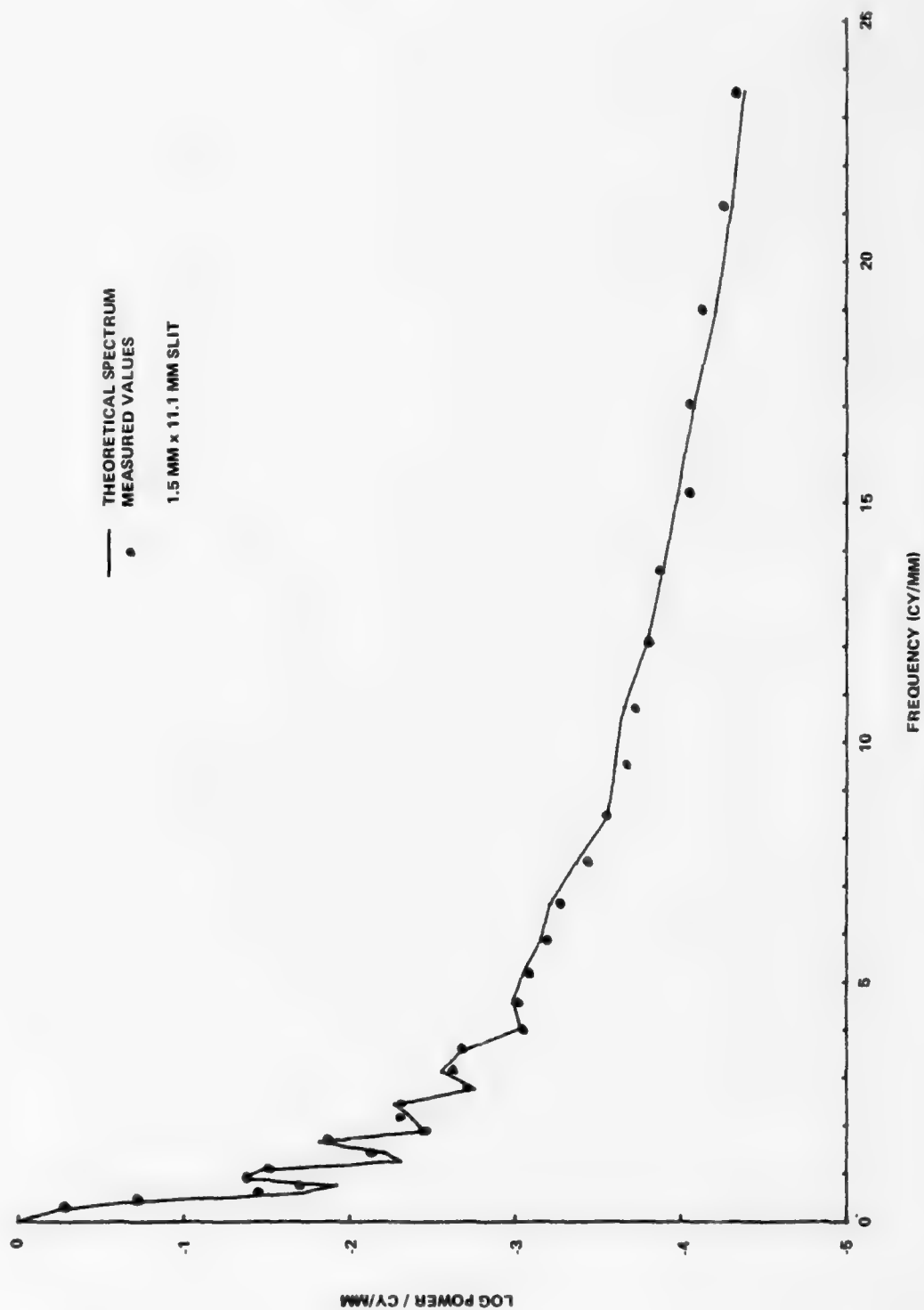Figure 7: Integrated Theoretical Spectrum

Figure 8: Measured Slit Spectrum

each of the individual elements. Values were generally of the order of 1% to 2% of the mean reading.

Wedge readings confirm the adequacy of the one-dimensional measurement. The wedge corresponding to the spike produced by the slit length was 3.2% of the wedge corresponding to the major direction of measurement. The repeatability of the wedges was consistent with the levels observed for the ring elements.

These results demonstrate the validity of the basic diffraction integral as expressed in equation (11). They also indicate that the measurement equipment is operating satisfactorily and that the data processing procedures are adequate for this application.

Two Dimensional Variation

Consider a clear circular aperture with diameter, d. Then,

$$R(X, Y) = \begin{cases} 1, & |X|, \ |Y| \le d/2 \\ 0, & elsewhere \end{cases}$$

As before, the T designation will be dropped since the aperture is fixed. The Fourier transform of this function is derived in most optics textbooks, (see References 2 and 11), and will not be repeated here. The result is the well known Airy pattern distribution. In polar coordinates this result can be stated as

$$F\ (k_r,\ \gamma) = F\ (0)\ \frac{2J_1(\pi d \sin\alpha/\lambda)}{\pi d \sin\alpha/\lambda} \tag{30}$$

where $\quad \alpha$ = the angle of diffraction

d = the diameter of the aperture

$J_1(\ )$ = first order Bessel function

$F(0)$ = zero frequency or "DC" amplitude.

From (B.1) in Appendix B,

$$\sin \alpha = k_r \lambda$$

and (30) can be rewritten as,

$$F(k_r, \gamma) = F(0) \frac{2J_1(\pi d k_r)}{\pi d k_r}$$

From (15),

$$P(k_r, \gamma) = \frac{\left| F(k_r, \gamma) \right|^2}{D} = \frac{\left| F(0) \frac{2J_1(\pi d k_r)}{\pi d k_r} \right|^2}{D}$$

where D is the area of the aperture.

Therefore, since,

$$P(0) = \frac{\left| F(0) \right|^2}{D}$$

then,

$$P'(k_r, \gamma) = \frac{P(k_r, \gamma)}{P(0)} = \left| \frac{2J_1(\pi d k_r)}{\pi d k_r} \right|^2 . \tag{31}$$

Equation (31) was integrated over the areas of the individual elements to derive the theoretically expected values for three circular apertures 1/4, 1/2, and 3/4 inches in diameter. Five repeated OPS measurements were made of each aperture with a 40 inch focal length transform lens. The mean readings were processed as shown in equation (26) and the results shown in Figures 9, 10, and 11 along with the theoretical curves. The most obvious point in the figures is the large deviations that occur at power levels below 1×10^{-6}. It appears that the dynamic range capabilities of the ROSA will not permit accurate measurement below this limit. Performance, however, is satisfactory over 6 orders of magnitude. The
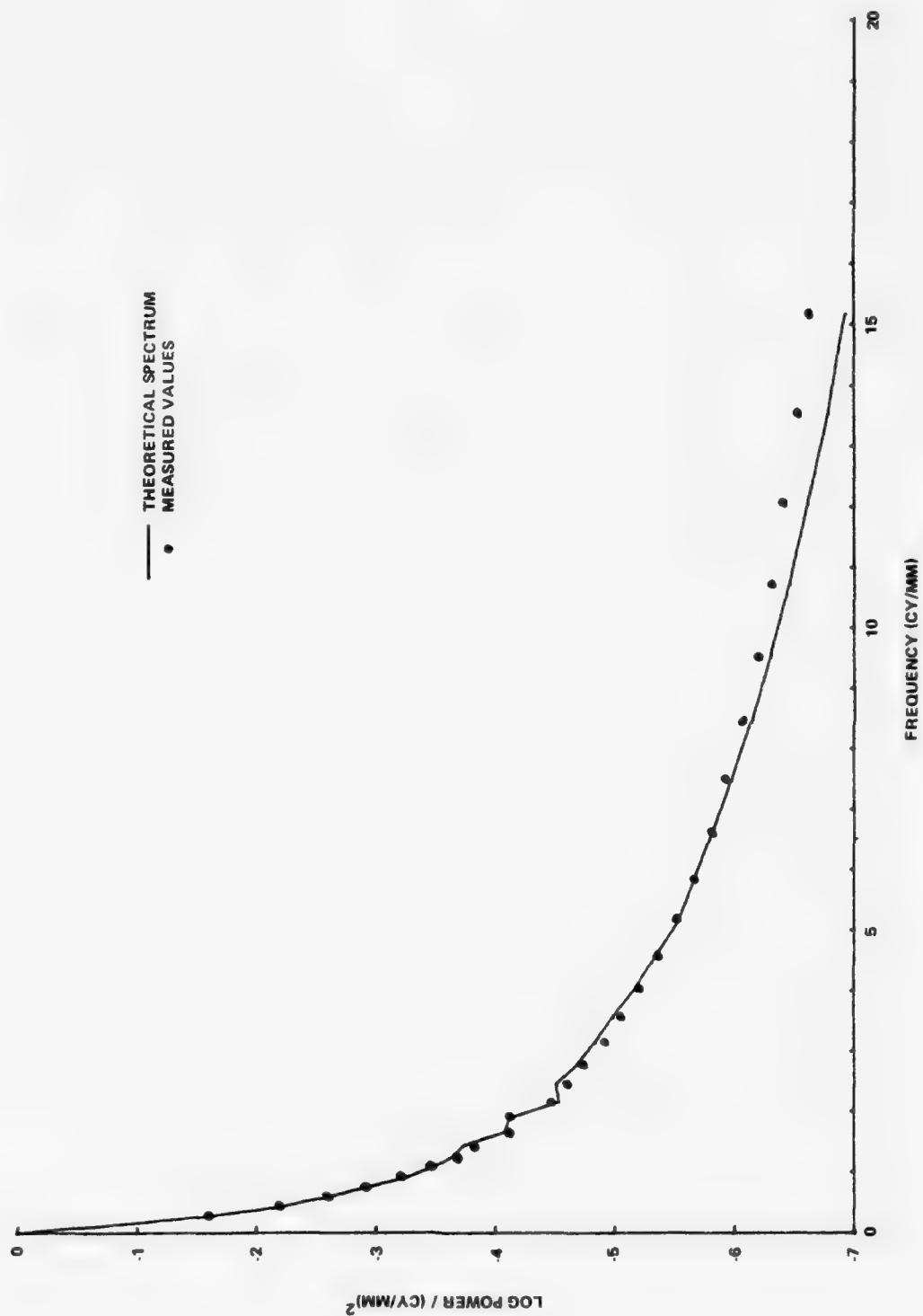
38

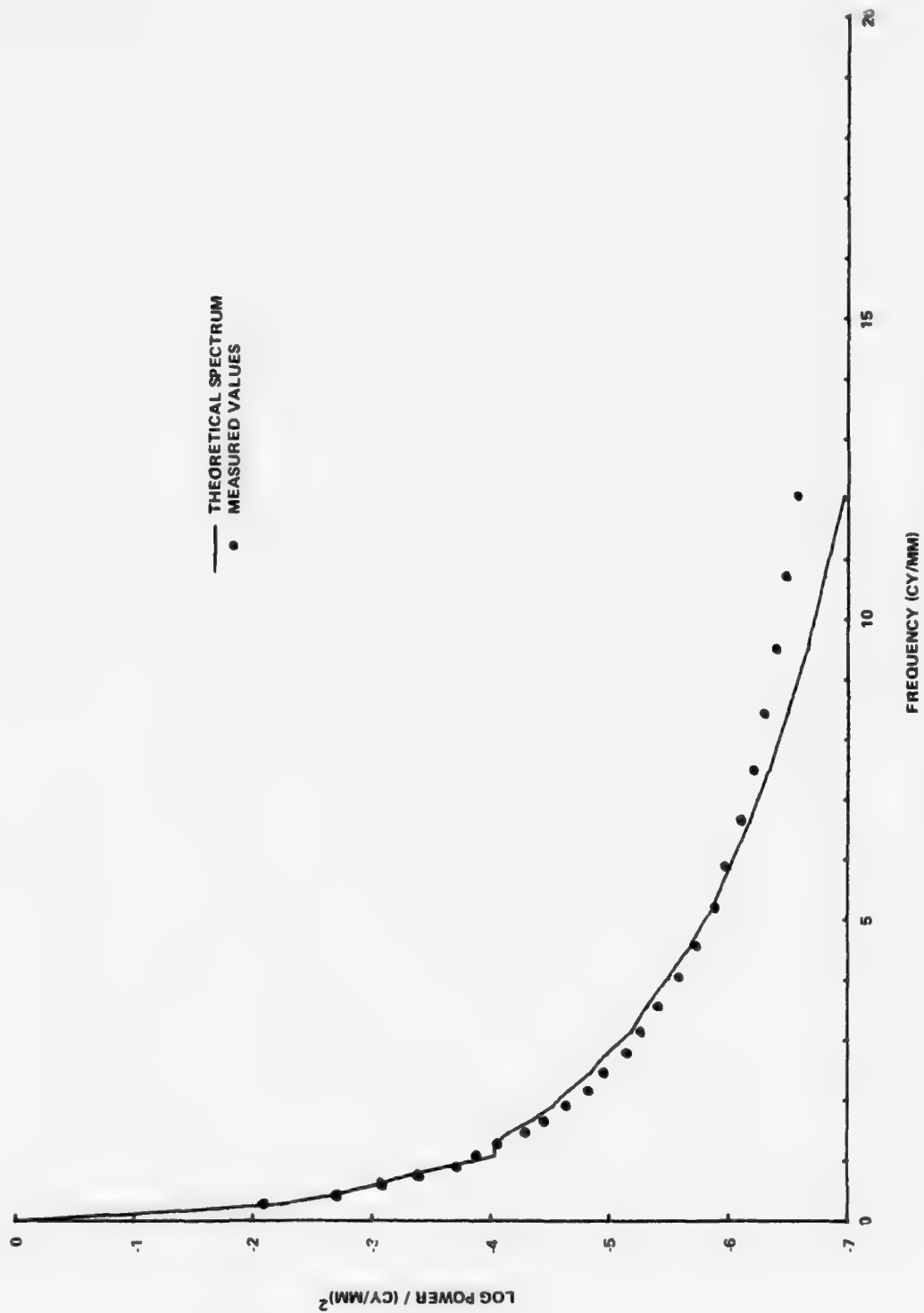Figure 9: ¼ Inch Diameter Circular Aperture
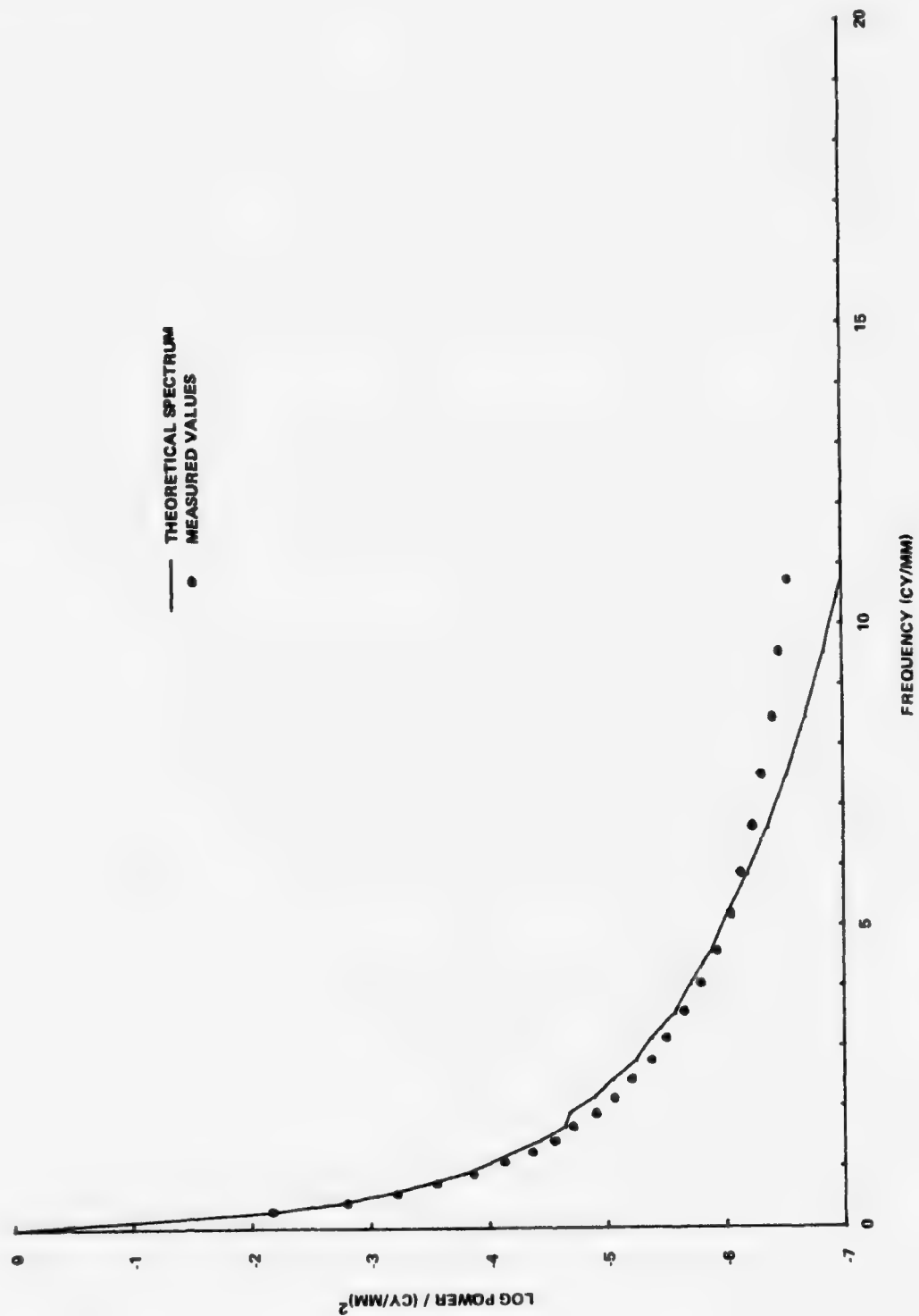
Figure 10: ½ Inch Diameter Circular Aperture

Figure 11: ¼ Inch Diameter Circular Aperture

root mean square error levels for values above 1×10^6 are about 10% for the 1/4 inch aperture and about 20% for 1/2 and 3/4 inch apertures. The very steep gradients in the diffraction pattern for the larger apertures present unusually difficult measurement problems. The 1/2 inch diffraction pattern intensity, for example, drops 6 orders of magnitude in a distance of less than 0.2 inches. Fortunately gradients of this magnitude rarely occur in practical applications and the 10% error level should be representative of system performance. The standard deviations for the repeated readings were consistent with those observed with the slit.

For the basic power spectrum measurements then, in both one and two dimensions, the equipment and data processing techniques can be expected to provide root mean square error levels of $\pm$ 10% and a repeatability error of $\pm$ 2% over a dynamic range of 6 orders of magnitude.

FILM INPUT MEASUREMENTS

The previous section dealt with the performance of power spectrum measurements of clear apertures. Most measurements of interest, however, will utilize photographic film as the input medium. Figure 12 presents an example of an OPS measurement of a photograph of a line grid. The grid, as measured on the photograph, had a frequency of 1.16 cycles/mm with a line (clear space) width of 0.37 mm. The one-dimensional theoretical spectrum can be expressed as, (after Reference 2),

$$P(k_x) = \left(\frac{\sin(\pi \omega k_x)}{\pi \omega k_x} \right)^2 \left(\frac{\sin(N\pi S k_x)}{\sin(\pi S k_x)} \right)^2$$

where ω = width of the clear spaces

S = width of one cycle

N = number of bars.

Comparison of the measured and theoretical spectra in Figure 12 indicates good agreement in shape, at least for the first five harmonics. The discrepancies,
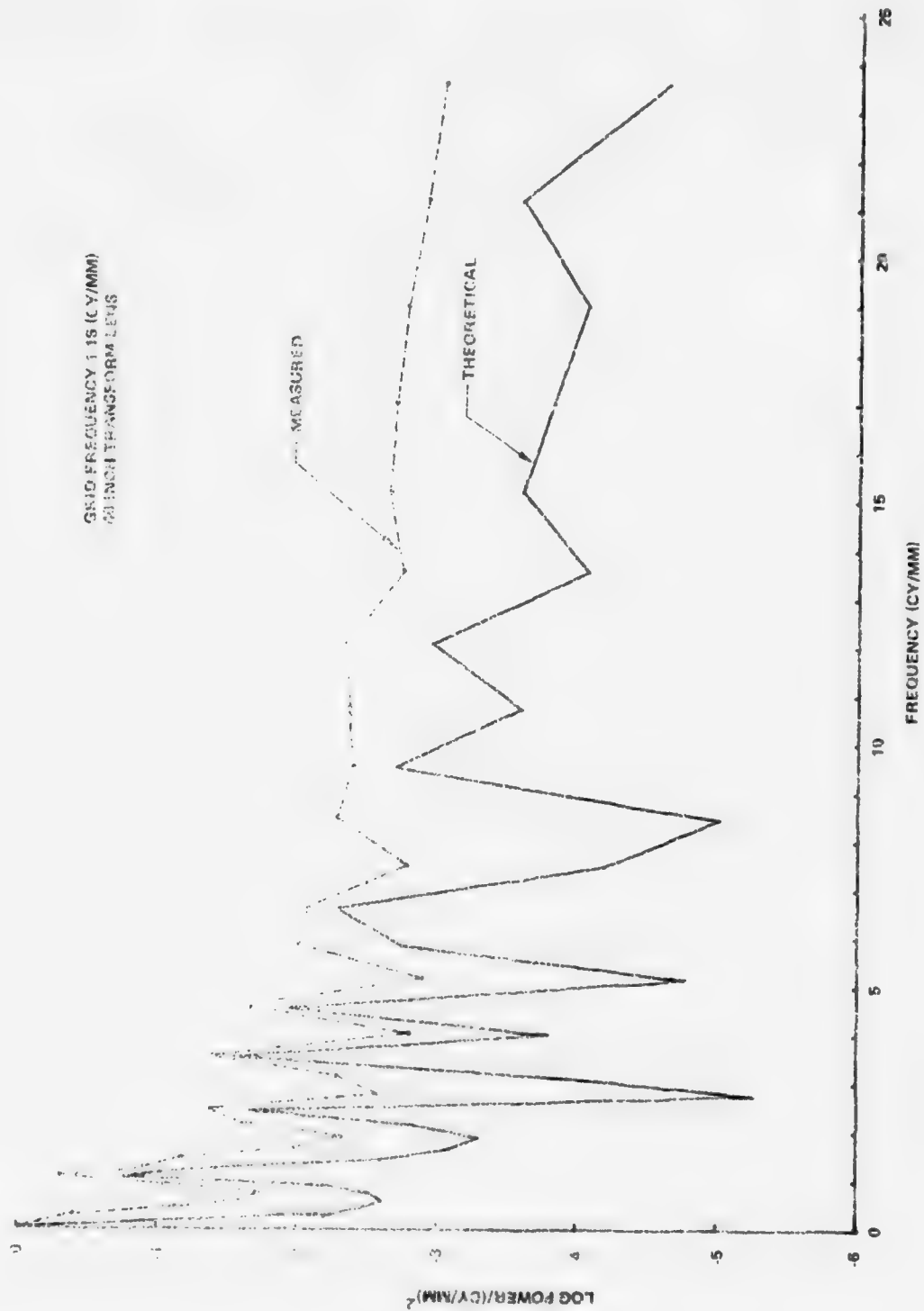
42

Figure 12: Line Grid Spectra

however, exceed the accuracy levels found for the clear aperture measurements.
The film imagery introduces several additional sources of error:

1. Nonuniformities in the thickness of the film base and emulsion
   introduce unwanted phase effects that distort the spectrum.

2. The aperture used to limit the measurement area in the film has an
   effect on the total power spectrum.

3. Film granularity introduces a noise effect.

4. Geometric distortion in the film introduces dimensional measurement
   errors.

5. The transfer characteristics of the camera-film combination modify
   the contrast, generally as a function of frequency.

These errors will be treated in greater detail in Phase II. However, a pre-
liminary test to evaluate the significance of the phase effects was performed
in this series.

As discussed in Section III, the optical power spectrum reflects the input am-
plitude distribution and as such is sensitive to phase effects introduced by
thickness irregularities. There are two sources for this problem; the variations
in the film base and the variations in the emulsion caused by the developed
image (image relief effects). The latter problem is the most serious since it
is "signal dependent" and cannot easily be measured independently.

Liquid gating is generally recommended to eliminate this problem (References 6,
7, 8, 9, 10). This technique involves immersion of the film sample in a liquid
of similar refractive index contained in a glass cell with optically flat sides.
Although there are some difficulties because the film base and emulsion generally
have different refractive indices, the technique is successful. However, it is
a cumbersome and time consuming procedure. The matching of refractive in-
dices must be done carefully and separately for each film type used. The errors
introduced by the liquid and the cell must be determined and removed. Because
of these problems it is important to determine the magnitude of the phase effects
and consider other approaches to compensate.

An image containing a number of bars of various sizes and orientations was mea-
sured and then bleached in photographic reducer to remove all of the developed
silver grains. The resulting image, although clear, retained the original
thickness variations. The image relief was clearly visible under reflected
light and in transmitted coherent light. Figure 13 compares the power spectra
of the original and bleached images. Both measurements were made with the lar-
gest possible aperture size, i.e., 3/4 inch and a 40 inch focal length transform lens.
Figure 14 compares the bleached image spectrum with that from a sample of clear
film. Although it is obvious that the image relief does contribute to the power
spectrum the difference is small when compared to original image power spectrum.
The difference between the bleached image spectrum and the clear image spectrum
is about 3% of the total image power levels except at very low frequencies
(< 0.5 cy/mm) where considerable spreading of the DC spot occurs with the clear
image. This comparison is not intended to be a definitive experiment, but it does
suggest that the use of a clear film sample for phase effects correction may be
sufficient for practical levels of accuracy. Such corrections are to be explored
and evaluated in Phase II of this study.

INFORMATION CAPACITY

The power spectrum provides the measurements required for the information capa-
city measure as defined in Section II, equation (10),

$$C = 4 \iint \log_2 \left[\frac{F_{S,N}(k_x,k_y,T)}{F_{\Delta R}(k_x,k_y,T)} \right] dk_x dk_y$$

From (11) in Section III

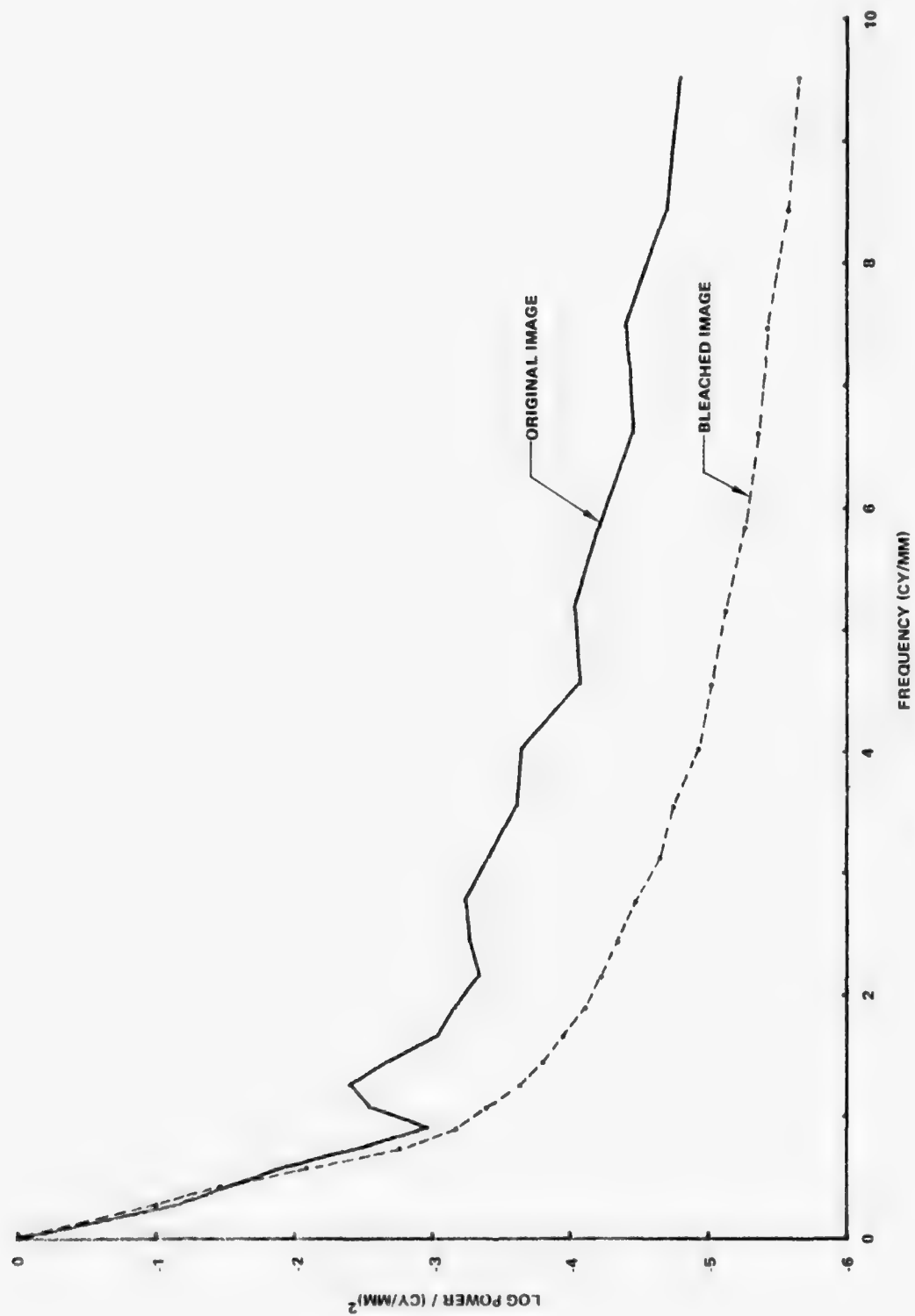$$P(k_x,k_y,T) = \frac{\left| F(k_x,k_y,T) \right|^2}{D} \; ,$$

and,

45

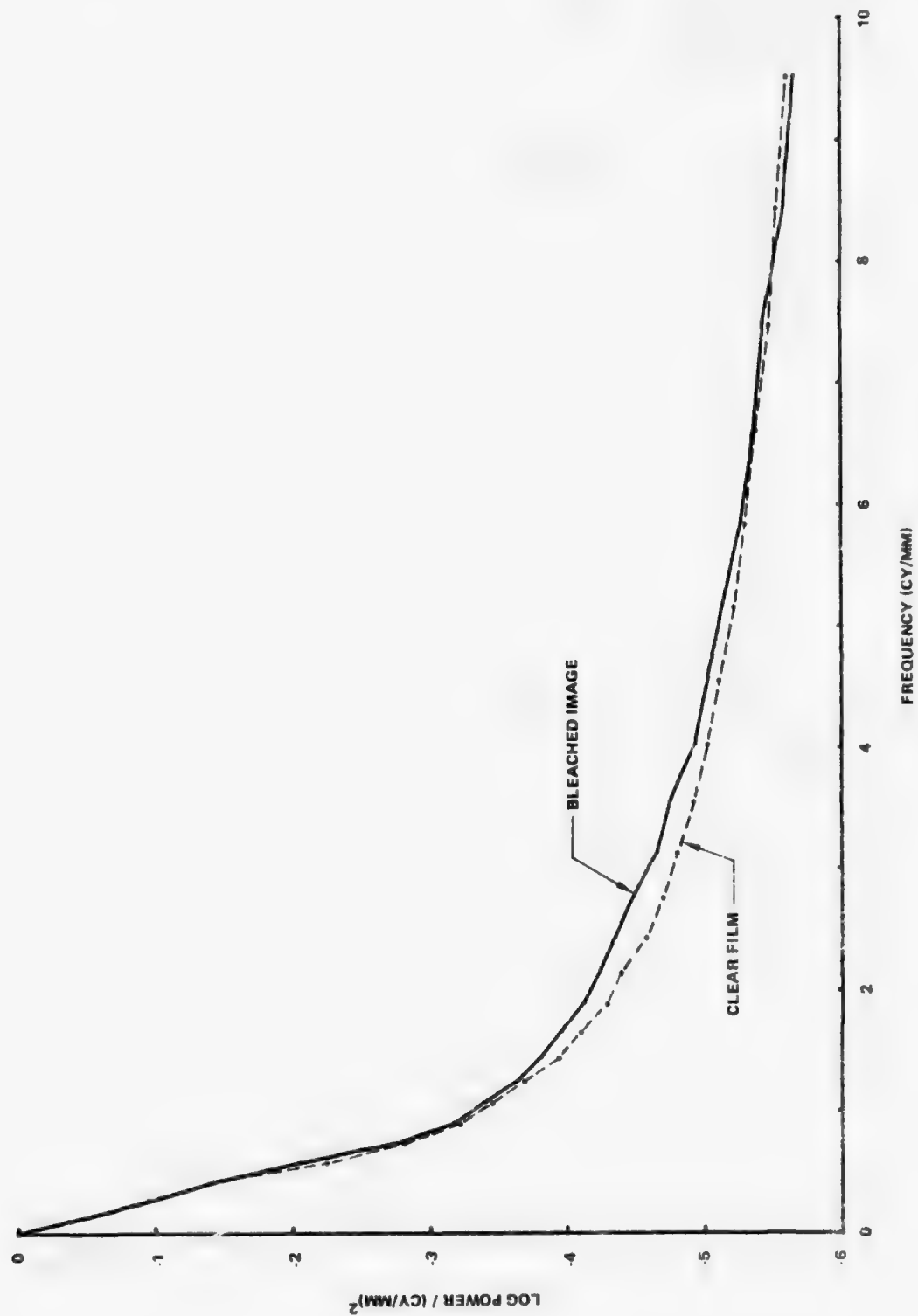Figure 13: Phase Effects (Original vs. Bleached)

46

Figure 14: Phase Effects (Bleached vs. Clear)

47

$$C = 4 \iint \log_2 \left[\frac{P_{S,N}(k_x,k_y,T)}{P_{\Delta R}(k_x,k_y,T)} \right]^{1/2} dk_x dk_y$$

$$= 2 \iint \log_2 \left[\frac{P_{S,N}(k_x,k_y,T)}{P_{\Delta R}(k_x,k_y,T)} \right] dk_x dk_y$$

where the upper limit of integration is the system cut-off frequency, K.

In polar coordinates,

$$C = 2 \iint \log_2 \left[\frac{P_{S,N}(k_r,\gamma,T)}{P_{\Delta R}(k_r,\gamma,T)} \right] dk_r d\gamma. \tag{32}$$

In order to evaluate the application of equation (32) a set of imagery was prepared using a computer controlled laser beam recorder. The recorder is a drum facsimile type controlled by a Varian 6201 computer which is responsible for timing and logical operations. Digital image data are provided via magnetic tape. The computer performs a gamma correction which compensates for nonlinearities in the printer modulator and film. The data are then converted to analog form to drive the laser modulator.

The imagery consists of nine frames with random dot patterns. The dots are 0.1 mm wide with 0.1 mm spacing. The frames represent three different numbers of grey levels (2, 4 and 16) each at three levels of dynamic range. The grey levels are printed at equal density intervals and are based on equal probabilities of occurrence. The steps are thus linear in density but have a log relationship with intensity and amplitude. All nine conditions were printed to the same density level. Table 3 lists the magnitude of the density steps for each condition.

Table 3: Grey Step Size (Density Units)

No. of Levels	Dynamic Range		
	High	Medium	Low
2	0.90	0.30	0.15
4	0.30	0.10	0.05
16	0.06	0.02	0.01

Table 4 defines the dynamic range conditions.

Table 4:   Levels of Dynamic Range

Range	Density Maximum	Minimum	Mean	Range
High	1.25	0.35	0.80	0.90
Medium	0.95	0.65	0.80	0.30
Low	0.88	0.72	0.80	0.16

A tenth frame was produced with a uniform signal at the same mean density level.

The film was Type 2405 XX, developed in D19 for 7 minutes at 70° F.   The printer calibration curves show a linear response over the maximum density range used (0.35D to 1.25D).

Optical spectrum measurements were made on all 10 frames using a 40 inch transform lens focal length and a 1 inch diameter circular aperture.   The resulting power spectra normalized to ring 1 are shown in Figure 15.   Except for the medium contrast-2 level frame, the spectra do not vary with the number of grey levels but are sensitive to dynamic range.   The spikes occur at the frequencies corresponding to the spacing of the dots.   The first spike occurs at about 10 cycles/mm corresponding to the inverse of the dot spacing at orientations of 0° and 90°.   The second spike is at 14.1 cycles/mm and represents the second harmonic of the diagonal sampling frequency.

The power spectra should not vary with the number of grey levels.   Power levels are a function of the input amplitude variance (mean square amplitude) and since the dot pattern grey levels have equal probability of occurrence the resulting distributions (rectangular) all have equal theoretical variance.   The discrepancy for the medium contrast-2 level frame is most likely attributable to physical alignment inaccuracies in the laser beam recording process.

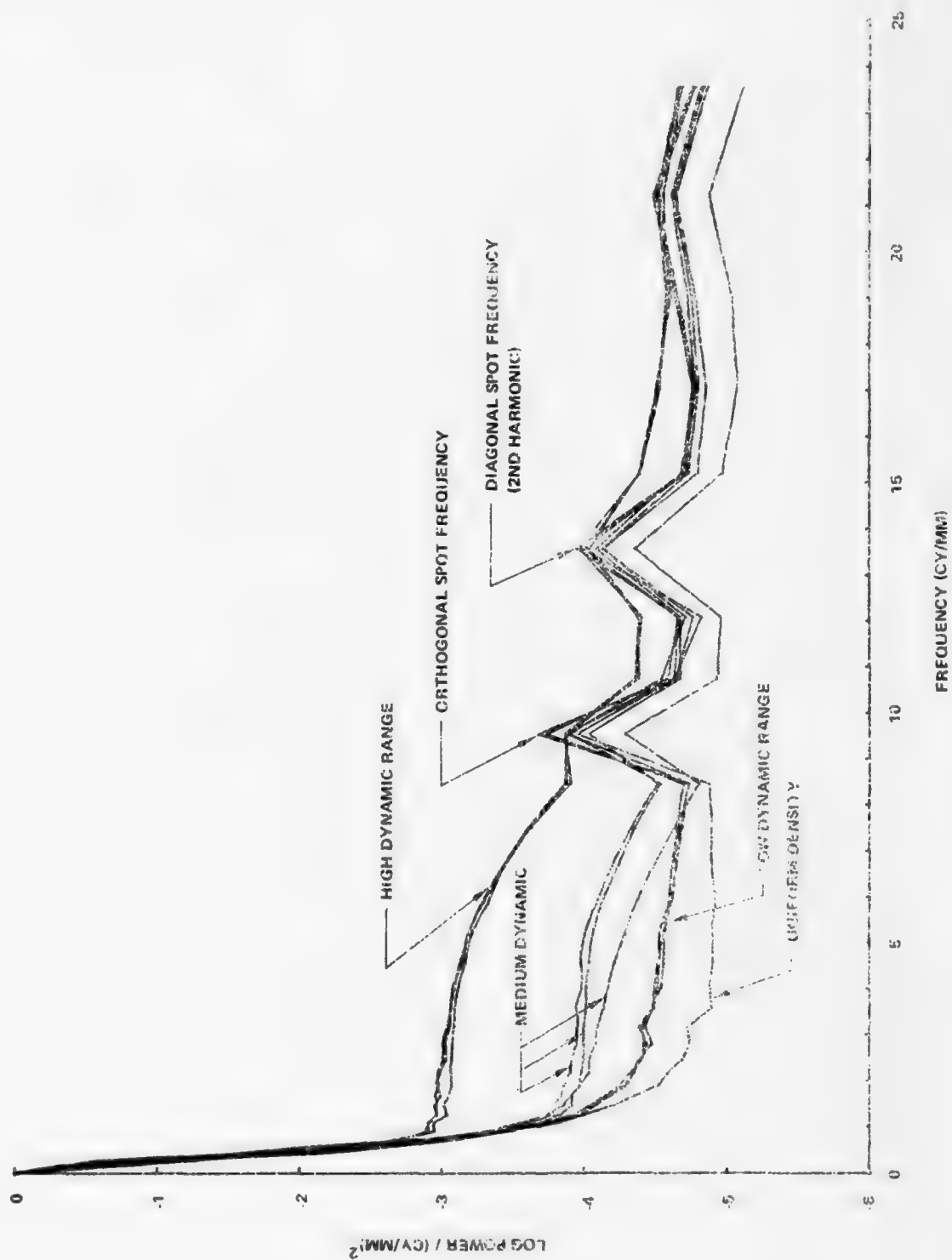The information capacity of the input signals can be calculated from equation (1),

49

Figure 15: Random Level Dot Spectra

$$C = \frac{N \log_2 i}{D},$$

where, for 1 square millimeter,

N = number of dots = 10^2 = 100
L = number of response levels (2, 4, or 16)
D = area = 1 mm^2.

Table 5 lists these results.

Table 5:   Information Capacity of Input Signals

Number of grey levels	Capacity (bits/mm^2)
2	100
4	200
16	400

The information capacity of the display (laser-film combination) can be determined as discussed in Section II by using the uniform density power spectrum as a measure of noise. Then for a noise limited display, we can define the just-discriminable response level in terms of the noise and equation (32) becomes

$$C = 2 \iint \log_2 \left[\frac{P'_{S,N}(k_r, y)}{P'_N(k_r, y)} \right] dk_r dy. \tag{33}$$

The prime designations have been added to indicate the use of normalized power spectra. Normalized spectra are not required if all measurements are made with the same laser amplitude and the same image mean transmission values. Although these conditions were controlled, normalized spectra were used here to correct for possible discrepancies. The T designation (integration time) has been dropped since this analysis involves a static display.

It is important to note that equation (33) defines the capacity of the display. It does not reflect the amount of information actually displayed. As with the

51

power spectrum, this measure should not vary with the number of grey levels in the signal but should be a function of the dynamic range. Capacity values were calculated for each of the nine frames using equation (33). The results are listed in Table 6. The value $K = \dfrac{1}{2 \times \text{dot spacing}} = 5$ cycles/mm was used as the upper limit of integration.

Table 6: Display Capacity Values (bits/mm^2)

Dynamic Range	Number of Input Grey Levels			Mean	S.D.
	2	4	16		
0.90D	282.1	288.7	289.1	286.6	3.9
0.30D	109.2	138.6	128.8	125.5	15.0
0.16D	54.2	56.6	53.2	54.7	1.8

The agreement across input levels is very good except for the discrepant frame. The mean capacity values vary as expected with dynamic range. If the dynamic range is expressed as modulation, the relationship between information capacity and dynamic range is nearly linear over the values measured.

$$M = \frac{T_{max} - T_{min}}{T_{max} + T_{min}}$$

where T_{max}, T_{min} are the maximum and minimum intensity transmission values.
T = antilog (-D).

This is shown in Figure 16. The amount of information for each of the three input levels is shown as dashed lines. The plotted values indicate that the display capacity is exceeded by the 16 level input at all levels of dynamic range. Capacity is exceeded by the 4 level input at the medium and low dynamic range levels and by the 2 level input by the low dynamic range level.

The preceding analysis demonstrates that the general behavior and reliability of the OPS information capacity measure support the validity of the basic approach.
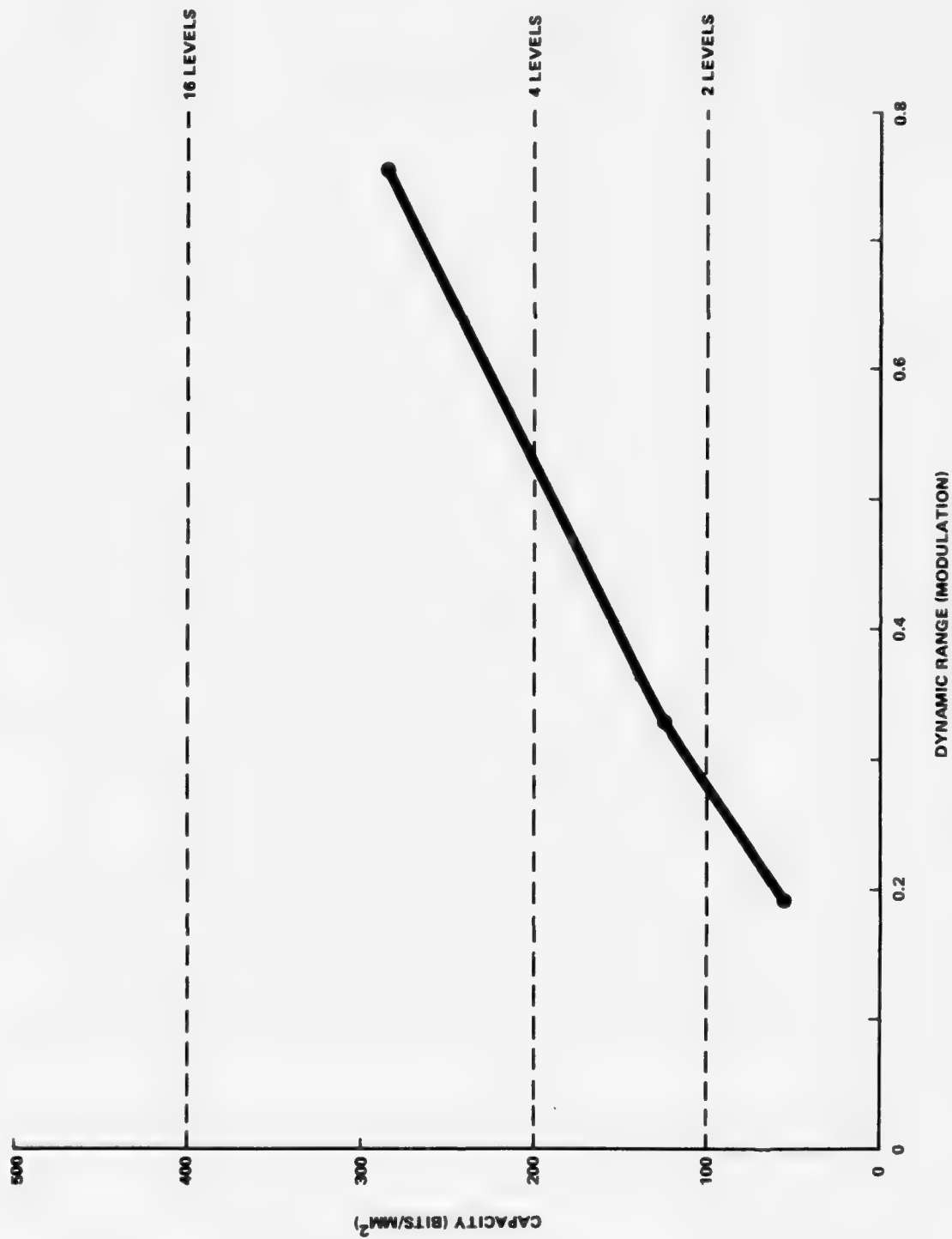
Figure 16: Dot Pattern Information Capacity

53

Consider the 4 grey level-high dynamic range conditon. From Figure 16, the input information level (200 bits/mm^2) is within the display capacity. From Table 3, the grey step size is 0.30D. Also from Table 3, the 2-level medium range condition represents a single grey step for the former condition. Thus,

$$C = 2 \iint \log_2 \left[\frac{P_{4H}(k_r,\gamma,T)}{P_{2M}(k_r,\gamma,T)} \right] dk_r d\gamma,$$

should equal the input information capacity, where

$P_{4H}(k_r,\gamma,T)$ = power spectrum measured on the 4-level high dynamic range condition.

$P_{2M}(k_r,\gamma,T)$ = power spectrum measured on the 2-level medium dynamic range condition.

Evaluation of the above equation provides a value for the output image informa-tion capacity of 180 bits/mm^2. This value compares favorably with the theore-tical value of 200 bits/mm^2.

54

SECTION V

IMAGE NOISE

INTRODUCTION

The use of the optical power spectrum for determining display information capacity is highly dependent on the proper measurement of image noise. When the display system is noise limited, the display noise power spectrum is a major component of the information capacity metric. A major requirement is that the noise measurement be truly representative of the form and magnitude of the noise actually present in the image of interest. The ease with which this requirement can be met is largely determined by the characteristics of the noise itself.

Power spectrum measurement of photographic noise has been extensively studied (see, for example, ref. 6 and 10). Photographic noise, principally granularity, is one of the least difficult types to evaluate. It is static, isotropic (equal in all directions), behaves in a reasonably predictable fashion and has been examined in great detail. This is in contrast to CRT display noise, for example, that is dynamic, differs significantly with direction, and is not well understood. There has been a great deal of work with noise in the CRT video signal; but much less is known about the resulting image noise on the CRT screen.

The following discussion considers those noise characteristics that are important for the proper measurement and use of the noise power spectrum in information capacity measures.

ADDITIVITY

The information capacity equation that uses the noise power spectrum as a direct signal-to-noise ratio,

$$C = 2 \iint \log_2 \left(\frac{P_{S, N}(k_x, k_y)}{P_N(k_x, k_y)} \right) dk_x \, dk_y \qquad (34)$$

is based on the assumption, among others, that the noise behaves in an

55

additive fashion. This means that the noise is added to the signal level.
Thus,

$$R_{S, N} (x, y) = R_{S} (x, y) + R_{N} (x, y)$$

and from the properties of the Fourier transform

$$F_{S, N} (k_x, k_y) = F_{S} (k_x, k_y) + F_{N} (k_x, k_y)$$

and since

$$P (k_x, k_y) = \frac{\left| F(k_x, k_y) \right|^2}{D}$$

$$
\begin{aligned}
D \, P_{S, N} (k_x, k_y) &= \left| F_{S, N}(k_x, k_y) \right|^2 = \left| F_{S} (k_x, k_y) + F_{N} (k_x, k_y) \right|^2 \\
&= \left| F_{S} (k_x, k_y) \right|^2 + 2 F_{S} (k_x, k_y) \, F_{N} (k_x, k_y) + \left| F_{N} (k_x, k_y) \right|^2 \\
&= D P_{S} (k_x, k_y) + D P_{N} (k_x, k_y) + 2 F_{S} (k_x, k_y) \, F_{N} (k_x, k_y)
\end{aligned}
$$

$$\tag{35}$$

If the noise is also independent of the signal, the cross-product term
(representing covariance) becomes zero and the power spectra are also additive.

If the display noise is multiplicative rather than additive; i.e.,

$$R_{S, N}(x, y) = R_{S}(x, y) \ R_{N}(x, y)$$

then it is the case that

$$F_{S, N} (k_x, k_y) = \left| F_{S} (k_x, k_y) \right| * \left| F_{N} (k_x, k_y) \right|$$

and

$$P_{S, N}(k_x, k_y) = \left[\left| F_{S} (k_x, k_y) \right| * \left| F_{N} (k_x, k_y) \right| \right]^2 \tag{36}$$

where * denotes the operation of convolution.

56

Equation (36) indicates a much more complex effect of noise on the power
spectrum and the use of equation (34) for information capacity measurement
is questionable. A theoretical solution for multiplicative noise does not
exist. If the errors introduced by the inappropriate use of equation (34)
are excessive, then modifications in the form of the equation will be
required. This concern is not limited to the optical power spectrum of in-
formation capacity; it applies to all applications of the signal-to-noise
ratio as a description of system performance.

SIGNAL DEPENDENCE

One aspect of the correlation between signal and noise has been mentioned above.
If a correlation exists, the cross product term in equation (35) does not
vanish and becomes a source of error. The magnitude of the error depends on
the size of the correlation.

Another, although related, difficulty occurs with the selection of a representa-
tive noise sample for measurement of the noise power spectrum. If the noise
is truly independent of the signal, then the noise will be identical at all
signal levels and any level of uniform signal input can be used to obtain an
appropriate noise spectrum. If, however, the noise level varies with the
signal level, the decision is more difficult. The common solution here is to
use the noise measurement at the image mean signal level. This may not be the
best choice, particularly if the relationship between signal level and noise
level is not linear. It is important, therefore, to evaluate the magnitude
and the form of the relationship and select the most appropriate conditions
for the noise measurement.

DIRECTIONALITY

If the magnitude or other characteristics of the noise vary with orientation
in the display, it becomes important to consider this effect in any evaluation.
There are two approaches to this problem. One is to use only input signals
that are directionally uniform. This will avoid the interaction between scene
content and noise. The other approach is to use an input signal with highly
directional content such as a grid pattern and obtain measurements over a range
of orientations. The latter approach will provide a quantitative evaluation of
the directionality effect.

DYNAMIC NOISE

If a display output varies with time, the effect of noise that is random with time will depend on the magnitude and rate of variation and on the integration time of the viewer or other sensor (such as photographic film). If the magnitude of the noise is described at any time t by its variance, then

$$\sigma^2_{N,t} = \frac{\sum (R_x - \overline{R})^2}{n-1}$$

where

R_x = the display response level at point x

$\overline{R}$ = the average response level

n = the number of display points sampled

If the noise is directional, sampling should be only in the direction of interest.

If the noise is random, then the response levels at each point in the display will be averaged over some integration time T. In general,

$$\sigma^2_{N,T} = \frac{\sigma^2_{N,t}}{n'}$$

where

n' = the number of time samples in the integration period.

For example, if f is the frame time for a CRT display, then

$$n' = \frac{T}{f}$$

Parseval's theorem states that

$$\int \left| f(x) \right|^2 dx = \int \left| F(u) \right|^2 du$$

For this application the above is interpreted to mean that the area under the square of the Fourier transform (i.e., power spectrum) is equal to the variance of the input. Hence a reduction in noise variance by a factor n' because of

58

integration will produce a reduction by the same factor in the area under the power spectrum. It may, therefore, be possible to derive the spectrum of the integrated input analytically.

The empirical approach is to perform the integration photographically (by control of exposure time) and perform the power spectrum measurement on the integrated signal. Both approaches are to be considered in Phase II.

EVALUATION

The magnitude of the effect of deviations from the assumptions of additive and independent noise is difficult to evaluate in the general case. To obtain some estimate of the potential error magnitude, a "worst case" condition was tested.

The effect of overprinting a "noise" pattern on a photograph is to produce multiplicative noise when measured as transmission. A test of such noise effects was performed using photographic transparencies of two high contrast line grids (1.16 cy/mm and 1.76 cy/mm), and two "noise" overlays. The overlays were produced by the laser recorder with a spot size and spacing of 0.2 mm. The spots varied in transmission according to a random Gaussian distribution. The mean transmissions of the two overlays were equal. They differed in root-mean-square deviation (high noise and low noise). The dot pattern of the overlays was aligned with the bars on the grid to produce a high spatial correlation between the bar signal and the noise. Optical power spectrum measurements were made of each of the grids, each of the overlays, and of each grid under both overlay conditions. The measurements were made with a 40 inch focal length lens and a 24 mm x 35 mm rectangular aperture. If the noise behaved like independent, additive noise, then in polar coordinates,

$$P_{S,N}(k_r, \gamma) = P_S(k_r, \gamma) + P_N(k_r, \gamma) .$$

For each of the grids the two-dimensional power spectra (integrated across γ) were calculated and used to evaluate this relationship. Figure 17 illustrates this evaluation for the 1.16 cy/mm grid and high noise condition.

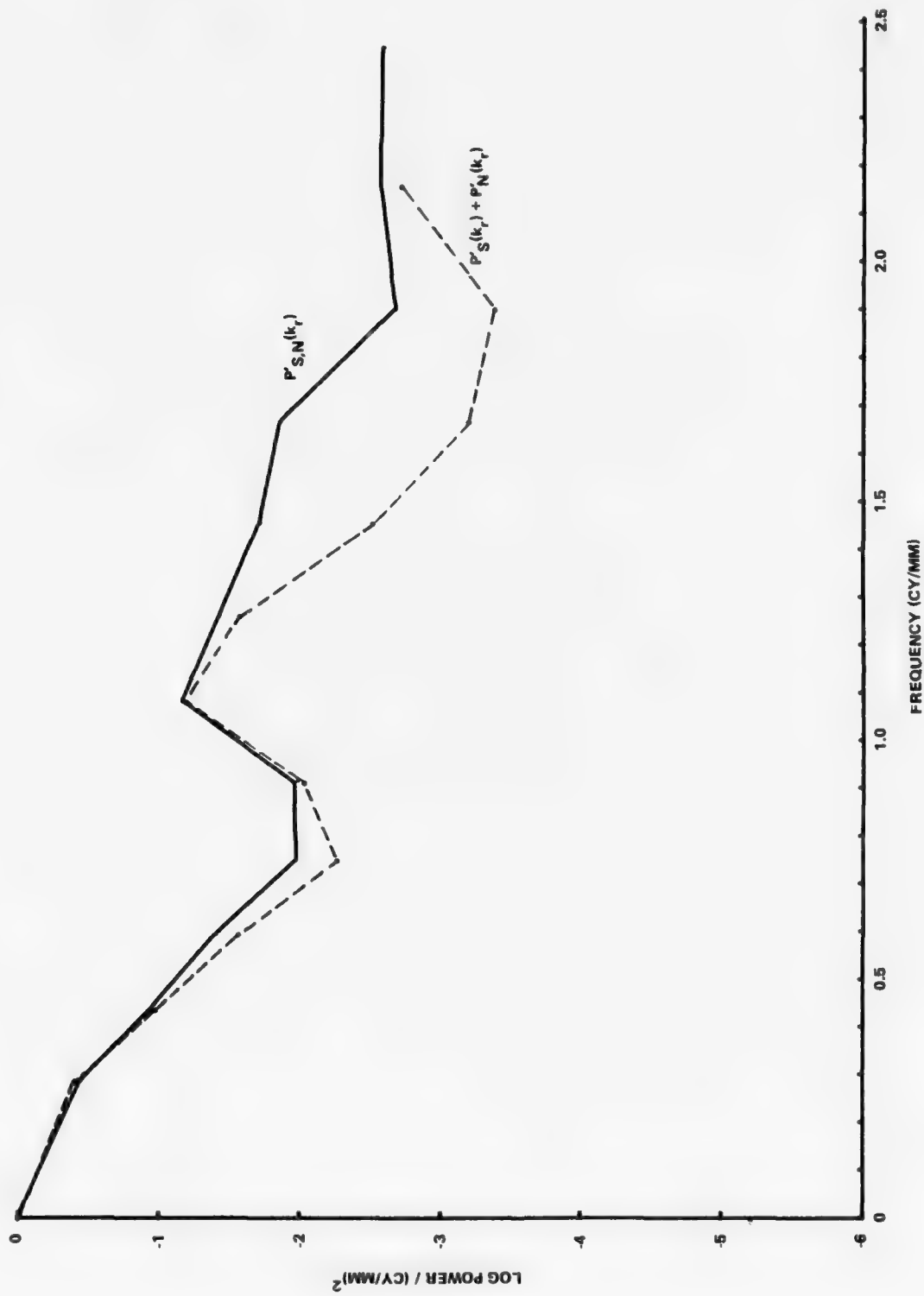The spectra were evaluated out to the cutoff frequency, K, where

Figure 17: Evaluation of Additivity

60

$$K = \frac{1}{2 \times \text{dot spacing}} = \frac{1}{2 \times .2} = 2.5 \text{ cy/mm}.$$

Figure 17 clearly shows that the simple sum underestimates the combined spectrum at the lower power levels although agreement is good at higher levels. The root mean square deviations from the combined spectrum were calculated for each condition and are presented in Table 7.

Table 7:   RMS Errors in Noise Additivity
(percent of composite value)

Grid Frequency	Noise Level	R.M.S. Deviation
1.16 cy/mm	Low	63%
1.16 cy/mm	High	50%
1.76 cy/mm	Low	55%
1.76 cy/mm	High	64%

The errors are fairly random. They do not appear to be dependent on noise level or grid frequency. The size of errors is surprisingly small considering the severity of the conditions imposed. Furthermore, the effect on information capacity measures will be somewhat less since the major deviations, at least in this case, occur at the lower power levels which in turn have the least effect on information capacity. The consistency of the magnitude and nature of the errors (underestimation at low power levels) also suggest the possible development of an empirical correction. Such an approach, however, will require much more detailed testing under more realistic conditions.

Based on the preceding results, there is reason to believe that for more realistic conditions the noise measurement errors will not be excessive. An evaluation like the one just discussed, however, should be performed for specific conditions of interest before such a decision is made. If such an evaluation demonstrates unacceptable error levels, an empirical correction can be considered or an alternate approach used.

ALTERNATE APPROACHES

The information provided by the wedge elements in the ROSA detector offers
some promise for alternate approaches. The wedges provide power values as a
function of orientation integrated over a frequency interval determined by
the detector geometry and the measurement optics (see equation (20) in
Section III. Figure 18 is a plot of the relative wedge values for the
1.16 cy/mm grid with the high noise condition. The input was oriented so
that the power spike from the grid falls at 90°. The two dimensional noise
pattern produces spikes at 0°, 90°, and 180° as well as on the diagonals,
45° and 135°. The 90° wedge, therefore, provides an integrated spectrum
for the combined noise and signal. Integrated noise spectra are provided
by the wedges at 0°, 45°, 135° and 180°. Unfortunately, the 0° and 180°
wedges do not fully cover the spikes and the 45° and 135° wedges provide
noise values along the pattern diagonal and are only relatively correct for
the effect at 90°. A 45° tip of the input image would have provided more
valid data. However for illustrative purposes signal-to-noise values for
each of the grid-noise combinations were calculated from

S/N = 90° wedge/45° wedge

These values are listed in Table 8, along with the same calculations from
measurements on the grid inputs with noise.

Table 8:   Wedge Signal-to-Noise Values

Grid Frequency (cy/mm)	Noise Overlay Level	90° wedge/45° wedge	Percent Loss
1.16	None	142.7	
1.16	Low	38.2	73.2
1.16	High	32.8	77.0
1.76	None	216.0	
1.76	Low	60.9	71.2
1.76	High	59.9	72.3

The percent S/N loss due to the overlay is also shown in the table. The
resulting values are consistent with expectations except for the small difference
between noise levels for the 1.76 cy/mm grid.

Figure 18: High Noise Wedge Values

63

The resulting values are of the form

$$\frac{\int P'_{S, N} (k_r, \gamma) \, d k_r}{\int P'_N (k_r, \gamma) \, d k_r}$$

and

$$\log_2 \frac{\int P'_{S, N} (k_r, \gamma) \, d k_r}{\int P'_N (k_r, \gamma) \, d k_r} \neq \iint \log_2 \left(\frac{P'_{S, N} (k_r, \gamma)}{P'_N (k_r, \gamma)} \right) d k_r \, d\gamma$$

The wedge signal-to-noise values, therefore, cannot be used directly in the information capacity metric but may well show a stable relationship with capacity.

This approach has an important advantage in that the noise measure is internal. The noise measure is, by definition, properly representative. Besides not being a direct measure of capacity, it has the additional disadvantage in that the input signal must be highly directional (e.g., a line grid). Furthermore, the present detector geometry does not provide a proper range of frequency integration. It is too large, for example, for the conditions in the test described above. This approach, however, remains a potential technique and merits further consideration in Phase II.

A second "indirect" capacity measurement approach using the wedge data can also be considered.

Figure 19 compares relative wedge values for the 1.16 cy/mm grid with and without the high noise overlay. It is intuitively reasonable to consider the magnitude of the relationship between these two spectra as an index of the "fidelity" of the noisy response. The correlation between these spectra (i.e., the input grid only and the output noise grid) provides such an index. Standard linear regression techniques as outlined in any statistical textbook will provide a best fit equation of the form
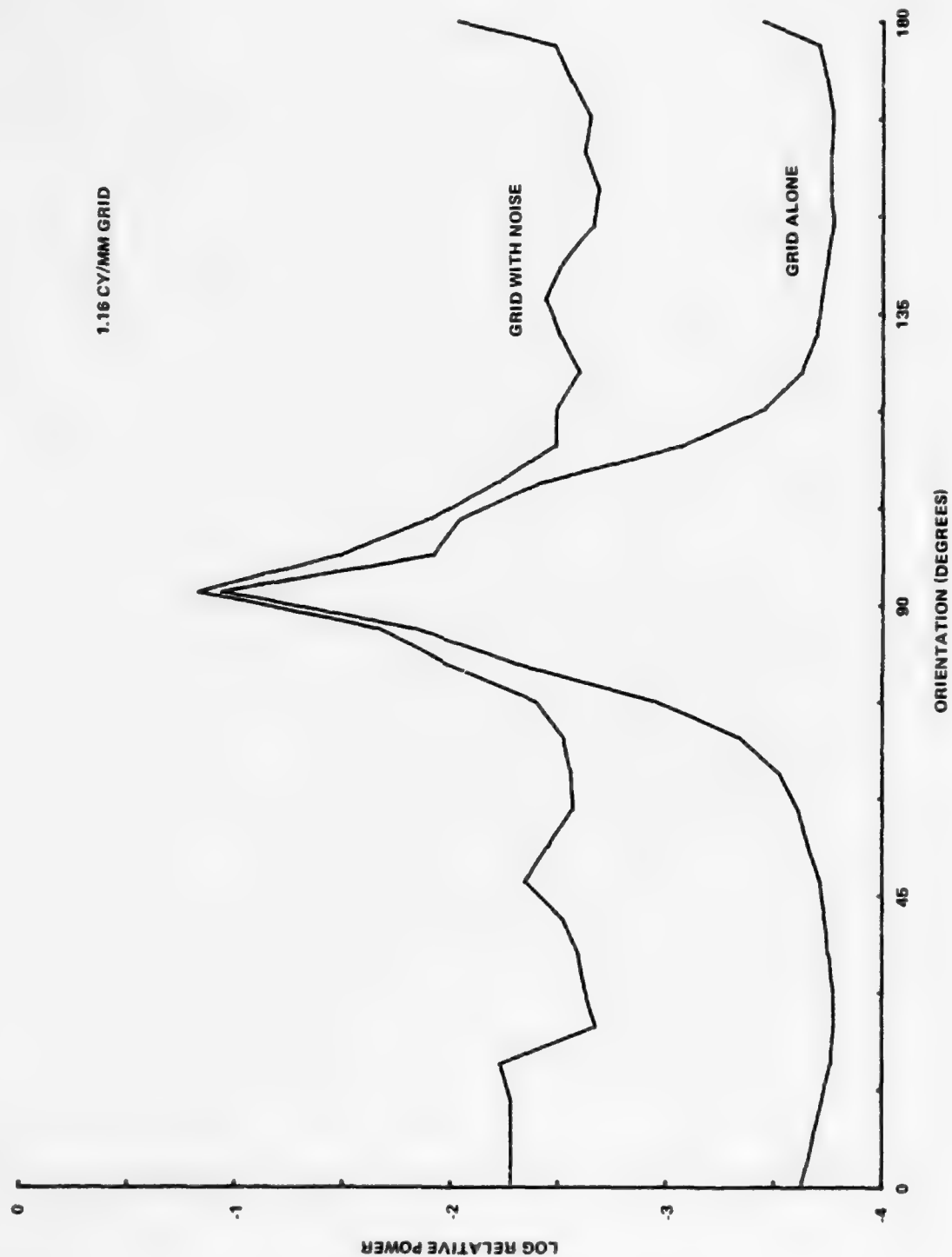
Figure 19: Comparative Wedge Values

65

$$W_{S,N}(\gamma) = A + B \, W_S(\gamma)$$

where

$W_{S,N}(\gamma)$ is the relative wedge value at orientation γ for the output image

$W_S(\gamma)$ is the corresponding value for the input image

This analysis provides two additional statistics that are relevant to display performance;

> The <u>coefficient of determination</u>, R^2, is the ratio of the variance in the independent variable ($W_{S,N}(\gamma)$) that is accounted for by the dependent variable ($W_S(\gamma)$). Conversely, $1 - R^2$ represents the proportion of the signal and noise spectrum that is unrelated to the signal. R^2, therefore, is a form of signal-to-noise ratio.

> The <u>standard error of estimate</u> is derived from R^2 and is the absolute value of the power in the signal and noise spectrum that is not related to the signal spectrum.

$$\text{S.E.E.} = \text{var}\,(W_{S,N}(\gamma))\,(1 - R^2)$$

The standard error of estimate, then, can be considered an internal measure of the noise component in the combined spectrum.

If, for the grid input, the 90° wedge value is used as an estimate of the combined spectrum, then an alternate signal-to-noise ratio can be defined as

$$\text{S/N} = \frac{90° \text{ wedge}}{\text{S.E.E.}}$$

The R^2 and S/N values were calculated for this "cross spectral correlation" approach and are listed in Table 9.

Table 9:   Cross spectral content for Series...

Grid Frequency (cy/mm)	Noise Overlay Level		
1.16	Low		
1.16	High		
1.76	Low		
1.76	High		

The R^2 and S/N values are mathematically ... agreement in trend. Both vary in the expect... lower values for the 1.76 cy/mm grid are ... the 45° wedge as a noise est... a selection between these two ...

Two approaches for obtaining ... defining and measuring a "represe... above. The "off-axis wedge" approach ... signal pattern. The "cross-... or measurement of the input ... some potential as display perform... further consideration in Phase ...

67

SECTION VI
DISPLAY PERFORMANCE EVALUATION

The preceding sections have dealt with the basic validity of a general approach for the measurement of display information capacity. The purpose of such a measurement is to provide a tool for the evaluation of viewer performance with imaging displays. A complete description of performance requires the determination of relationships between levels of relevant system parameters and information capacity. It is important, therefore, to identify those system parameters that are likely to influence information capacity.

The development of the basis approach has identified a number of display system parameters that will have an effect on the optical power spectrum measurements and hence on the resulting information capacity value.

SPATIAL FREQUENCY

Spatial frequency is a principal dimension in the optical power spectrum measurement. The capability to determine display output as a function of spatial frequency is an important property of this technique. The contributions, as a function of spatial frequency, to total display information capacity should be a useful discription of display performance. This distribution will be very sensitive to the display modulation transfer function.

DYNAMIC RANGE

Testing discussed in Section IV has shown the information capacity measure to be sensitive to maximum available contrast. The important parameter here is maximum contrast available to the viewer. Thus, degradations such as those caused by reflections of ambient light must be included. The image capacity vs. dynamic range distribution will indicate the sensitivity of a given display to such degradations.

DISPLAY LUMINANCE

Average luminance of the display will not have a direct effect on the information capacity measurement because of zero frequency normalization. However, the interaction of luminance with other parameters such as dynamic range or modulation transfer will be reflected in the measurement. An important interaction, for example, exists among all three parameters for the CRT displays.

Increased luminance usually improves the dynamic range but, since it also
tends to increase scanning spot size, will degrade the modulation transfer
function. Luminance vs. information capacity should identify optimum lumi-
nance levels for a given display.

INTEGRATION TIME

Visual integration will tend to reduce the effect of noise in dynamic displays.
This factor is important to proper measurement. Ideally, this should not be a
parameter. It is a characteristic of the viewer and if fixed and known would
be incorporated in the measurement process. Unfortunately, our knowledge of
visual integrative behavior is not adequate to achieve such an approach.
Measurement at a range of values around 0.1 seconds and correlation of results
with viewer performance should help identify a proper value.

CONTENT ORIENTATION

Directional effects will occur if the noise behavior and/or modulation transfer
vary with direction. This is likely to occur with line-scan CRT displays.
It is generally recommended that pictorial display resolution be equal in the
x and y directions. This recommendation should also apply to information
capacity. Matrix displays will exhibit reduced performance on the diagonals.
Information capacity measures can help to evaluate the magnitude of this degra-
dation.

NOISE

Noise level is another major parameter in the capacity metric. Noise character-
istics are often assumed to be fixed for a given display. Noise level will, of
course, vary with some of the parameters mentioned above. This effect should be
incorporated in the measurement, provided an appropriate noise sample is used.
It may, nevertheless, be of interest to evaluate the effect of additional, ex-
ternally imposed, noise levels on display performance. In this instance, noise
level would appropriately be used as a parameter and the resulting capacity vs.
noise level distribution used to evaluate, say, the susceptibility to jamming.

INPUT CHARACTERISTICS

The information capacity of the input signal will influence the measured display
capacity. Clearly, if the input level does not exceed the capability of the dis-
play, then display capacity has not been measured. Certain input characteristics

such as randomness and directionality have been discussed with respect to
their effect on capacity measurement and their utility as calibration or
measurement inputs.

If the measured *information* capacity is greater (at all frequencies) than
the levels of the information to be displayed, then the display is rated
high. If the capacity is not sufficient, then it is rated low. Such a
judgment requires knowledge of the information content of the range of in-
puts for the application of interest.

VIEWER CAPABILITIES

The most meaningful evaluation must encompass consideration of both display
and viewer capabilities. The viewer's performance is the ultimate criterion
and its interaction with the display parameters must be considered. Visual
integration time has already been discussed. Viewing distance is incorpor-
ated in the capacity metric when spatial frequency is expressed as cycles/
degree. A third area, contrast detection thresholds, has been mentioned in
Section II. This is a much more difficult situation. Its effect can be
minimized by dealing only with conditions where display noise is the limit-
ing parameter but the problem cannot be ignored and must involve a compari-
son between capacity measures and viewer performance.

In addition to thresholds, there is the problem of viewer information capa-
city. There is little advantage to a high display information capability if
it overloads the viewer. Our knowledge of visual information handling capa-
bilities is meager. The existence of a valid, reliable information capacity
measure would be a useful tool for extending this knowledge.

70

a) The general approach of optical power spectrum measurement for the determination of display information capacity is valid at the basic level.

b) The basic measurement capabilities of the existing OPS measurement equipment and calibration procedures are adequate. Root-mean-square (R.M.S.) deviations from theoretical values are about 10%. R.M.S. measures of repeatability error are about 2% of the expected value. These error levels apply over a useful dynamic range of 6 orders of magnitude.

c) There are a number of potential problems in the practical application of the general approach.

   o Nonlinearity of amplitude units
   o Measuring aperture effects
   o Phase effects
   o CRT film recording
   o Noise measurement

d) Promising solutions for these problems exist, but most need further development and testing.

e) The combined influence of the display and viewer characteristics on information capacity will include at least the following:

   o Spatial frequency response
   o Dynamic range
   o Luminance
   o Integration time
   o Input image characteristics
   o Noise
   o Viewing distance

INFORMATION THEORY

DEFINITION OF IFORMATION

A formal definition of "information" exists within the framework of information theory. This definition is a precise and unique measure and differs in some important respects from common understanding of information. Information theory does not deal with the meaning or relative importance among various pieces of information. It does not deal with the formation of concepts or decisions by the operator. The theory defines information as a change in the state of knowledge. To illustrate, suppose a display is provided to indicate the winner in a ten horse race. If all horses have an equal probability of winning, then before the race the state of knowledge can be described as the probability of identifying the winner;

$$\text{prob (initial)} = 1/10 = 0.1$$

At the end of the race the display indicates the winner and, if we know that the display is error-free, our state of knowledge is now perfect, i.e.;

$$\text{prob (final)} = 1.0.$$

The gain in knowledge or information is defined as;

$$\text{gain in information} = \frac{\text{prob (final)}}{\text{prob (initial)}}.$$

For this display;

$$\text{gain} = \frac{1.0}{0.1} = 10.$$

Suppose a simpler display were provided, one capable of indicating only whether the number, 1 through 10, of the winning horse was odd or even. Then, the displayed information reduces the number of possible winners to five and the resulting state of knowledge,

$$\text{prob (final)} = 1/5 = 0.2.$$

The resulting gain in information provided by the display;

$$\text{gain} = \frac{0.2}{0.1} = 2.$$

The gain in information is equal to the number of possible equiprobable display responses.

$$\text{prob (final)} = M/N_T$$

where,   M = number of possible display responses
         N_T = number of possible event outcomes.

$$\text{prob (initial)} = 1/N_T$$

and

$$\text{gain} = \frac{\text{prob (final)}}{\text{prob (initial)}} = \frac{M/N_T}{1/N_T} = M = 1/P$$

where P = probability of a given display response.

This is in agreement with the gain values calculated for the two displays above.

The basic unit of information is defined as the "bit" (short for binary digit). A bit is the amount of information provided by the answer to a yes-or-no question when both answers had an equal a priori probability of occurring. This is equivalent to the amount of information provided by the odd-even display above. For equal probability of occurrence the information, in bits, provided by a given display response is defined as;

$$H(R) = \log_2 \text{(gain)} = \log_2 M = \log_2 1/p \qquad\qquad (A.1)$$

For the examples above;

73

$$\text{...} \quad \log_2 \text{...} = 1.32 \text{ bits/response}$$

$$\text{"...} \text{...} \text{ display } H = \log_2 2 = 1.0 \text{ bits/response}$$

NON-EQUAL RESPONSE PROBABILITIES

Suppose a device is capable of displaying a series of responses where the set of possible responses is defined by,

$$R_1, R_2, R_3, \ldots, R_i, \ldots R_M$$

with probabilities of occurrence,

$$\ldots \quad p(R_2), \quad p(R_3), \ldots, p(R_i), \ldots, p(R_M).$$

Then if there is no statistical correlation between successive responses (zero-memory), the information gain from the display of R_i is $\log_2 1/P(R_i)$. Since the probability of this response occurring is $p(R_i)$, the average information gain per response, $H(R)$, will be:

$$H(R) = \sum_{i=1}^{M} p(R_i) \log_2 1/P(R_i) \tag{A.2}$$

$$= -\sum_{i=1}^{M} p(R_i) \log_2 p(R_i)$$

Shannon (Reference 12) proved that equation A.2 is maximized when the response probabilities are equal. Thus from equation A.1,

$$H(R)_{max} = \log_2 M \tag{A.3}$$

Maximum display information occurs when response probabilities are all equal to $1/M$.

NON-ZERO MEMORY

If correlations exist between successive responses a more complex description of display performance must be used. A Markov model is appropriate for such situations. An mth order Markov chain describes a situation wherein the occurrence of a response depends on some number, m, of previous responses but is independent of those occurring $m + 1$ or more responses earlier. The probability of the ith response, R_i, occurring after some particular sequence of m responses, is written as $p(R_i|m)$. This conditional probability will have a defined value for each possible previous sequence of m responses, and similar probabilities will be defined for all the other R responses. The information gain will be determined by summing for all responses over all previous m sequences:

$$H(R) = \sum_m \sum_i p(m, R_i) \log_2 1/p(R_i|m)$$

$$= \sum_{m+1} p(m, R_i) \log_2 1/p(R_i|m)$$

The last expression follows because summing over all m and i for sequences of m followed by R_i is equivalent to summing over all $m + 1$ sequences. It follows from the proof of expression A.3 that

$$\sum_{m+1} p(m, R_i) \log_2 1/p(R_1|m) \leq \sum_i p(R_i) \log_2 1/p(R_i) \leq \log_2 M \qquad (A.4)$$

Total equality holds for a zero-memory sequence with equal response probabilities. The left hand equality holds for all zero memory sequences. Maximum display information results when the display responses have equal and independent probabilities of occurrence and is equal to $\log_2$ (number of possible responses).

To illustrate these concepts, consider a display that provides a sequence of alphabetic symbols such as a teletype. Suppose the display is operating with

75

English text. The English language does not provide for equal or independent probabilities of occurrence of individual symbols. Some letters occur more frequently than others and the probabilities of occurrence depend on the specific sequence of preceding letters. High order Markov analyses of the English language are extremely difficult. However, a limiting value of about 1.6 bits per letter has been estimated for the information   (Reference 1). If the symbols (26 letters plus a space) were not restricted by the rules of English and occurred with equal and independent probabilities, then

$$H(R) = \log_2 M = \log_2 27 = 4.7 \text{ bits per letter.}$$

Thus, a teletype with 27 possible responses can provide information at a maximum rate of 4.7 bits per response. When the information is in the form of English text, however, the actual rate is about 1.6 bits per letter. This difference is not a function of the display's capabilities but is a result of the particular information coding scheme used (i.e., English text).

CAPACITY

For a sequential display such as a teletype, the information capacity is time related. If M(T) represents the number of responses (symbols) displayed in time T seconds, then capacity in symbols per second is

$$\text{CAPACITY} = \frac{M(T)}{T}$$

From expression A.4 maximum information capacity (optimum coding) in bits per second will be

$$C = \frac{\log_2 M(T)}{T} \tag{A.5}$$

Information theory, quite properly, expresses the relationship above as

$$C = \underset{T \to \infty}{\text{LIMIT}} \ \frac{\log_2 M(T)}{T}$$

The use of the limit is to require that M(T) be measured over a sufficiently long time period to insure an adequate description of display performance. This is especially important if the time required for individual symbols is not the same for all symbols (e.g., Morse Code).

We will drop the limit designation in subsequent expressions with the understanding that a proper measurement of capacity will involve sufficient sampling to represent all display responses of interest.

APPLICATION TO PICTORIAL DISPLAYS

Information in pictorial displays is presented in a parallel rather than sequential fashion. The individual responses are arranged in a spatial rather than a time sequence. Furthermore, the spatial arrangement of pictorial displays is generally two-dimensional as contrasted to the one-dimensional time sequence. For such two-dimensional spatial cases we can replace the time dimension with area in equation A.5.

$$C = \frac{\log_2 M(D)}{D} \qquad\qquad (A.6)$$

Capacity is expressed as bits per unit area on the display. The number of different intensity patterns of area D that can be reliably distinguished on the display is M(D).

The simplest case is that of a matrix of N cells such as an LED matrix display where each cell may be on or off. The number of different possible patterns, M is given by

$$M = 2^N$$

Dividing by the area of the matrix we have as an expression for the maximum capacity of the display

$$C = \frac{\log_2 M(D)}{D} = \frac{\log_2 2^N}{D} = \frac{N}{D}$$

The result shows that capacity is simply related to the number of elements. This is expected since each element having only two possible responses (on or off) provides 1 bit of information.

A more complex situation results if each element in the matrix can assume any one of a number L of intensity values. Then

$$M = L^N$$

and

$$C = \frac{\log_2 L^N}{D} = \frac{N \log_2 L}{D} \qquad (A.7)$$

APPENDIX B
OPTICAL POWER SPECTRUM MEASUREMENT

APPROACH

There are two basic approaches to the measurement of the power spectral density of an image. Historically, the most common approach involves the measurement of the image intensity distribution, $I(x,y)$, usually with a scanning microdensitometer. The autocorrelation function of the resulting data is calculated and Fourier transformed to produce $F(k_x, k_y)$. The modulus or real part of the Fourier transform is then squared to produce the power spectrum. This approach is time consuming and expensive, particularly if a two-dimensional spectrum is required. To meet sampling requirements, an extensive scanning operation is required. The computer requirements (capacity and time) for Fourier transformation of a very large data matrix are not insignificant.

An alternative approach involves the use of coherent optical processing. This approach takes advantage of an important property of coherent illumination. Under proper conditions, an aperture illuminated with coherent light produces a diffraction pattern that is related to the power spectral density of the aperture. With this approach it is possible to sample large areas rapidly and to measure the power spectrum directly without the need for a large computer capability. This approach is called optical power spectrum measurement and is the one used in this study.

FRAUNHOFER DIFFRACTION

The conditions necessary for the measurement of optical power spectra are those required for the production of a Fraunhofer diffraction pattern. When a beam of light passes close to the edge of an obstacle some bending of the light occurs. All such departures from the rectilinear propagation of light are called diffraction. The diffraction of the illuminating plane waves as they pass through a grating is shown in Figure B-1. The equiphase lines represent the cylindrical surfaces of the diffracted waves. As these waves continue beyond the grating, their equiphase surfaces tend to blend together and

79

look more and more like plane wave fronts. These apparent plane waves form
moving in several directions. The largest plane wave (not shown here) forms
moving along the optical axis. This is the zero order wave. The next largest
waves travel in directions determined by the grating line spacing and the
light wavelength. The constructive interference of part of the light diffrac-
ted down by the grating is shown in the figure. The path lengths from consecu-
tive grating apertures to a plane perpendicular to the direction of the wave
differ by one wavelength. This would be a first order wave. There is also a
similar wave diffracted up. Second order waves are formed by the construc-
tive interference of light with aperture path lengths differing by two wave-
lengths.

As shown in Figure B-1, the angle of diffraction, α, is related to the wave-
length, λ, and the line frequency, k, by the formula

$$\text{Sin } \alpha = \lambda k \qquad\qquad (B.1)$$

for

$$- \pi/2 < \alpha < \pi/2$$

A plane wave diffracted by a line grating forms a series of plane waves mov-
ing off at angles predicted by the above formula. As shown in Figure B-2,
a plane wave passing through a lens is focused to a spot in a plane located
one focal length behind the lens. The diffraction pattern formed in this plane
is called the Fraunhofer diffraction pattern. The position (r) of the spot
in the focal plane (Fraunhofer Diffraction Plane) is taken into account by the
equation

$$\tan \alpha = \frac{r}{F}$$

where F is the focal length of the lens.

Since, from equation (B.1)
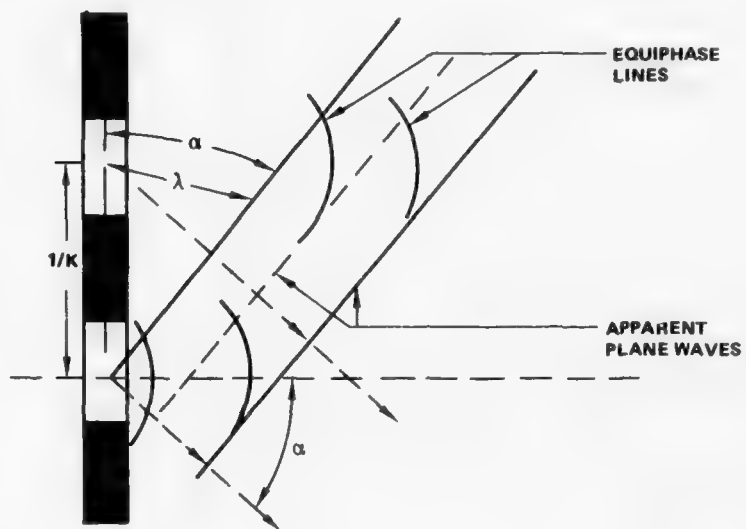
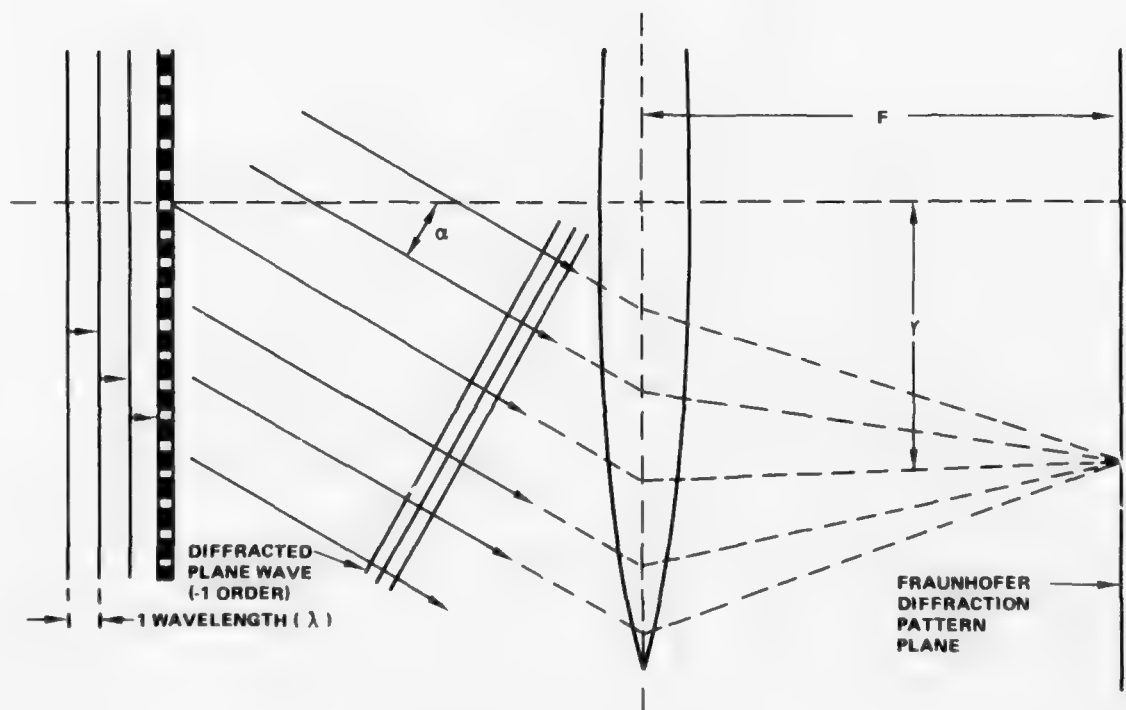$$\text{Sin } \alpha = \lambda_k$$

80

Figure B-1: Diffraction Geometry

Figure B-2: Fraunhofer Diffraction

81

and

$$\sin \alpha \cong \tan \alpha \text{ for } |\alpha| < 10^0 \qquad (B.2)$$

$$r = F\lambda k$$

Therefore a spatial frequency k in the input image will cause light to be concentrated in the diffraction plane at a radius equal to $F\lambda k$. The output position is only a function of the diffracted angle. It is independent of x, y position in the input plane but is sensitive to orientation.

THE DIFFRACTION INTEGRAL

The light amplitude at any point in the Fraunhofer diffraction pattern is proportional to the Fourier coefficient for the corresponding spatial frequency component.

Specifically,

$$A(\ell,m) = \frac{1}{\lambda F} \iint A(x,y) \exp\left[-2\pi i/\lambda \, (\ell x + my)\right] dx \, dy \qquad (B.3)$$

where   l and m are angular coordinates defined by the diffraction angles
$(\ell = \sin \alpha_x; \; m = \sin \alpha_y)$
$A(\ell,m)$ is the diffraction pattern amplitude distribution
λ is the wavelength of the coherent illumination
F is the focal length of the transform lens.

The limits of integration are defined by the input image area. The derivation of equation (B.3) is somewhat lengthy and will not be treated here. The topic is covered in most standard optical texts. References 2 and 11 are recommended.

$A(x,y)$ is the amplitude distribution in the input plane. It can be expressed as

$$A(x,y) = LA_T(x,y) \qquad (B.4)$$

82

where L = the amplitude of the coherent illumination (assumed to be constant over the image area)

$A_T(x,y)$ = amplitude transmittance distribution at the input image plane.

So,

$$A(\ell,m) = \frac{L}{\lambda F} \iint A_T(x,y) \exp\left[-2\pi/\lambda \ (\ell x + my)\right] dx\ dy \qquad (B.5)$$

From B.1

$$\ell = \sin \alpha_x = \lambda k_x, \text{ and}$$
$$m = \sin \alpha_y = \lambda k_y$$

and

$$A(r_x,r_y) = \frac{L}{\lambda F} \iint A_T(x,y) \exp\left[-2\pi i(k_x x + k_y y)\right] dx\ dy \qquad (B.6)$$

where r_x and r_y are linear dimensions in the diffraction plane,

$$r_x = \ell/F, \text{ and}$$
$$r_y = m/F.$$

The integral is the Fourier transform of $A_T(x,y)$ so,

$$A(r_x,r_y) = \frac{L}{\lambda F} F_T(k_x,k_y). \qquad (B.7)$$

The amplitude distribution of the diffraction pattern, however, cannot be measured directly. Photodetectors measure intensity, I, rather than amplitude. Since

$$I = |A|^2$$

the practical application of (B.7) can be written as

$$I(r_x, r_y) = \frac{L^2}{\lambda^2 F^2} \left| F_T(k_x, k_y) \right|^2 .$$

For the dynamic image case where the response function is expressed as

$$A_T(x, y, T),$$

$$I(r_x, r_y) = \frac{L^2}{\lambda^2 F^2} \left| F(k_x, k_y, T) \right|^2 . \qquad (B.8)$$

REFERENCES

1. Dainty, J. C. and Shaw, R. Image Science - Principles, Analysis, and Evaluation of Photographic-Type Imaging Processes. Academic Press, 1974.

2. Ditchburn, R. W. Light. 2nd Edition, Interscience Publishers, 1963.

3. Frieden, B. R. Information, and the Restorability of Images. J. Opt. Soc. Amer., April 1970, 60, 575-576.

4. Shaw, R. The Application of Fourier Techniques and Information Theory to the Assessment of Photographic Image Quality. Photo. Sci. & Eng., 1962, 6, 281-286.

5. Parsons, J. R. and Tescher, A. G. The Cross-Spectrum Error Criterion as an Image Quality Measure. Aerospace Corp. Report ATR-74 (8139)-1, Sept. 1973.

6. Thiry, H. Power Spectrum of Granularity as Determined by Diffraction. J Photo. Sci., 1963, 11, 69-77.

7. Thiry, H. Spectrometric Measurement of the Acutance of Photographic Materials. J. Photo. Sci., 1963, 11, 121-131.

8. Vander Lugt, A. and Mitchel, R. H. Technique for Measuring Modulation Transfer Functions of Recording Media. J. Opt. Soc. Amer., 1967, 57, 372-379.

9. Stark, H., Bennett, W. R. and Arm, M. Design Considerations in Power Spectra Measurements by Diffraction of Coherent Light. Applied Optics, 1969, 8, 2165-2172.

10. Vilkomerson, D. H. R. Measurements of the Noise Power Density of Photo-sensitive Materials at High Spatial Frequencies. Applied Optics, 1970, 9, 2080-2087.

11. Smith, F. G. and Thomson, J. H. Optics. John Wiley & Sons, 1971.

12. Shannon, C. E., A Mathematical Theory of Communication, Bell Syst. Tech. J., 1948, 27, 379.